

Learning Minimal Neural Specifications

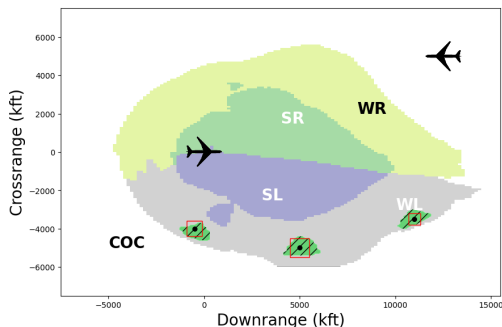
CHUQIN GENG, McGill University, Canada
 ZHAOYUE WANG, McGill University, Canada
 HAOLIN YE, McGill University, Canada
 XUJIE SI, University of Toronto, Canada

Formal verification is only as good as the specification of a system, which is also true for neural network verification. Existing specifications follow the paradigm of *data as specification*, where the local neighborhood around a reference data point is considered correct or robust. While these specifications provide a fair testbed for assessing model robustness, they are too *restrictive* for verifying any unseen test data points – a challenging task with significant real-world implications. Recent work shows great promise through a new paradigm, *neural representation as specification*, which uses neural activation patterns (NAPs) for this purpose. However, it computes the most refined NAPs, which include many redundant neurons. In this paper, we study the following problem: Given a neural network, find a minimal (general) NAP specification that is sufficient for formal verification of the network’s global robustness. Finding the minimal NAP specification not only expands verifiable bounds but also provides insights into which set of neurons contributes more to the model’s robustness. To address this problem, we propose three approaches—conservative, statistical, and optimistic—each offering distinct trade-offs between efficiency and performance. The first two rely on the verification tool to find minimal NAP specifications. The optimistic method efficiently estimates minimal NAPs using adversarial examples, without making calls to the verification tool until the very end. Each of these methods offers distinct strengths and trade-offs in terms of minimality and computational speed, making each approach suitable for scenarios with different priorities. The learnt minimal NAP specification allows us to inspect potential causal links between neurons and the robustness of state-of-the-art neural networks, a task for which existing work fails to scale. Our experimental results suggest that minimal NAP specifications require much smaller fractions of neurons compared to the NAP specifications computed by previous work, yet they can significantly expand the verifiable boundaries to several orders of magnitude larger.

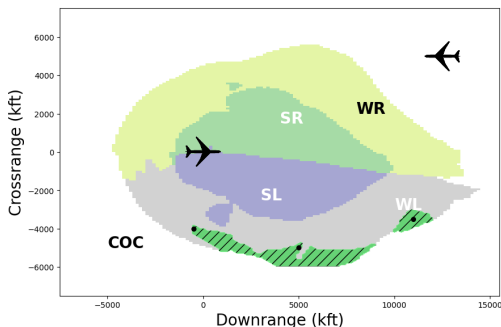
1 INTRODUCTION

The growing prevalence of deep learning systems in decision-critical applications has elevated safety concerns regarding AI systems, such as their vulnerability to adversarial attacks [Dietterich and Horvitz 2015; Goodfellow et al. 2015]. Therefore, the verification of AI systems has become increasingly important and attracted much attention from the research community. The field of neural network verification largely follows the paradigm of software verification – using formal methods to verify desirable properties of systems through rigorous mathematical specifications and proofs [Wing 1990]. A notable trend in existing works [Huang et al. 2020, 2017a; Katz et al. 2017b, 2019; Wang et al. 2021b] focuses on scaling verification to larger and more complex neural networks. While scalability is undeniably important and requires the collective effort of the research community, this paper explores an orthogonal angle that has been largely overlooked: *defining meaningful specifications*.

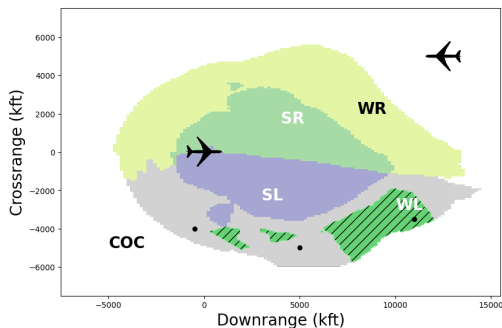
To illustrate, nearly all existing works follow a “*data as specification*” paradigm, where the specification is defined by the consistency of local neighborhoods—often L_∞ balls—around reference data points. While local neighborhood specification provides a fair and effective testbed for evaluating neural network robustness, it primarily covers a tiny convex region of input data that can mathematically be described by adding noise to the reference point, as illustrated by the red bounding box in Figure 1a. This small region is constrained by its adversarial examples. It is too restrictive to adequately address a broader, unseen test set, which are real data sampled from the underlying distribution.



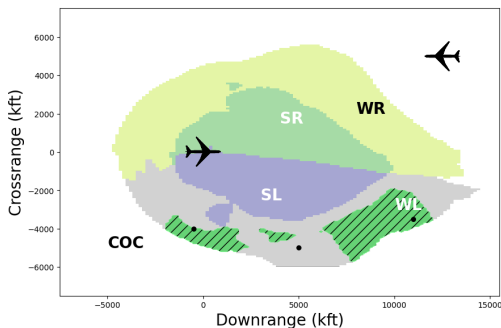
(a) Local neighborhood as specifications of the 3 reference points compared to using NAP as specification, NAP learnt from the 3 reference points and their local neighborhoods. Covers 4.23% and 7.64% of the WL region respectively.



(b) NAP as specification, NAP learnt from the 3 reference points. Covers 10.61% of the WL region.



(c) NAP as specification, NAP learnt from data points in the entire WL region. Covers 26.36% of the WL region.



(d) NAP as specification, with NAP learnt from the entire WL region and coarsened. Covers 32.43% of the WL region.

Fig. 1. Illustration of verifiable regions of the Weak Left (WL) region of the ACAS_Xu [Katz et al. 2017a] advisories for a head-on encounter with $a_{prev} = \text{Clear of Conflict (COC)}$, $\tau = 0s$. The red bounding boxes represent the verifiable regions when using data as specifications, constrained by the reference points and their adversarial examples. The green hatched areas denote verifiable regions when using Neural Activation Patterns (NAP) as specifications.

Ideally, the specification should produce a verifiable region that includes all data points from the same class, where the data points may be distributed in a non-linear and non-convex manner within the input space. For instance, consider the safety-critical Airborne Collision Avoidance System for Unmanned Aircraft (ACAS Xu), the neural network processes an input representing the state of the aircraft and outputs one of five advisories: Clear of Conflict (COC), Weak Left (WL), Strong Left (SL), Weak Right (WR), or Strong Right (SR). Observe in 1 the the inputs belonging to Weak Left (WL) depicted in grey forms a irregular shape. This complexity underscores the need for flexible and robust specifications capable of accurately capturing such intricate distributions. Unlike local neighborhood specifications, manually defining such a specification is impractical. This poses a tricky chicken-egg problem: machine learning (ML) is necessary because it's challenging to formally write down a precise definition (aka specification); but to be able to verify machine learning models,

a formal specification would be needed. We argue that, in order to tackle this challenge, a separate learning algorithm for specifications is necessary. In this view, the “*data as specification*” paradigm is a simple but extremely overfitted algorithm for specification learning, which simply picks a small neighborhood of a reference data point in the input space. To this end, Geng et al. [2023] proposes using a new and more promising paradigm - “*neural representation as specification*”, which learns a specification in the representation space of the trained machine learning model in the form of neural activation patterns (NAPs). NAPs are value abstractions of hidden neurons which have been shown useful for understanding the inference of a model [Gopinath et al. 2018]. Most importantly, a well-trained neural network would exhibit similar activation patterns for input data from the same class, regardless of their actual distance in the input space [Bengio et al. 2013; Geng et al. 2023; Tishby and Zaslavsky 2015]. This key observation suggests that if we learn a NAP—a common activation pattern shared by a certain class of data—it can serve as a candidate specification for verifying data from that class. Once such a NAP specification is successfully verified, we say any data covered by this NAP (exhibiting this pattern) provably belongs to the corresponding class. Ideally, if that NAP covers all data from a class, it can be considered a machine-checkable definition of that class. Geometrically speaking, compared to the L_∞ ball specifications, NAP specifications provide greater flexibility, enabling coverage of larger and more irregular regions. This advantage is particularly notable when reference points are near the boundaries of the WL region as illustrated in Figure 1a. In 1b we observe that the common NAP learned from the three reference points covers a significantly larger region compared to the combined coverage of the individual NAPs learned from each reference point independently. 1c demonstrates even greater coverage when the NAP specification is learned from all inputs belonging to the WL class.

However, it is noteworthy that the current approach to computing NAPs relies on a straightforward statistical method that assumes each neuron contributes to certifying the robustness of neural networks. Consequently, the computed NAPs are often overly refined. This is a restrictive assumption, as many studies [Frankle and Carbin 2019; Liang et al. 2021; Lu et al. 2019; Wang et al. 2021a] have shown that a significant portion of neurons in neural networks may not play a substantial role. In the spirit of Occam’s Razor, we aim to systematically remove these redundant neurons that do not impact robustness. This motivates us to address the following challenge: given a neural network, how can we identify a minimal NAP (i.e., the coarsest abstraction) that is sufficient for verifying the network’s robustness? This problem is important for the following reasons: i) Minimal NAP specifications cover potentially much larger regions in the input space compared to the most refined ones, enhancing the ability to verify more unseen data; ii) Minimal NAP specifications provide insight into which neurons are responsible for the model’s robust predictions, helping to uncover the black-box nature of neural networks. For instance, if we aim to decode NAPs into human-understandable programs or rules [Li et al. 2023], minimal NAPs will always be easier to interpret than larger NAPs. We leave the interpretation of individual neurons as future work.

To find the minimal NAP specifications, we first introduce a basic algorithm, COARSEN, which exhaustively checks all possible candidates using off-the-shelf verification tools, such as Marabou [Katz et al. 2019]. Specifically, COARSEN gradually coarsens each neuron in the most refined NAPs, retaining only the coarsened neurons when Marabou confirms verification success. While this approach provides correctness guarantees, it is not efficient for verifying large neural networks, as calls to verification tools are typically expensive. To improve efficiency, we further propose statistical variants of COARSEN—namely, STOCHCOARSEN, which leverages sampling and statistical learning principles to find minimal NAP specifications. 1d highlights that coarsened NAP specifications, which involve fewer neurons, can cover an even larger portion of the WL region, highlighting the effectiveness of coarsened specifications in achieving broader coverage of the complex input space.

However, verification-dependent approaches face challenges in scaling up to state-of-the-art neural network models due to the limitations of current verification tools. To address this, we develop an optimistic method, OPTADVPRUNE, which leverages adversarial examples to identify essential neurons—the fundamental building blocks of minimal NAPs. Our experimental results show it can efficiently estimate an initial starting point for minimal NAP specification and only making calls to the verification tool until the very end. We further apply these methods to state-of-the-art neural networks, such as VGG-19 [Simonyan and Zisserman 2014]. While formal verification of these estimated minimal NAP specifications remains impractical due to current scalability constraints in the underlying verification engine, we demonstrate that these NAPs capture significant hidden features and concepts learned by the model. As many studies suggest, visual interpretability and robustness are inherently related, emerging in learned features and representations [Alvarez Melis and Jaakkola 2018; Boopathy et al. 2020]. Consequently, we believe that the identified essential neurons contribute to the model’s robustness, and their activation states can serve as empirical indicators of confident predictions. Our contributions can be summarized as follows:

- We introduce the problem of learning minimal NAP specifications, emphasizing the need for a new paradigm in neural network specification. We present three approaches, each offering distinct trade-offs between efficiency and performance.
- We define key concepts such as the abstraction function, NAP specification, and essential neurons. We demonstrate that the problem reduces to identifying essential neurons and propose an optimistic approaches for estimating them.
- We propose a simple yet effective method for estimating the volume of the region mapped by the NAP. Our experiments show that minimal NAP specifications extend the verifiable bound by several orders of magnitude.
- We estimate essential neurons in the state-of-the-art VGG-19 network. Using a modified Grad-CAM map, we show that these essential neurons contribute to visual interpretability, providing strong evidence that they may also explain the model’s robustness.

2 BACKGROUND

In this section, we introduce basic knowledge and notations of adversarial attacks and neural network verification, with an emphasis on verification using NAP specifications. This may help readers better understand the importance of learning minimal NAP specifications.

2.1 Neural Networks for Classification Tasks

In this paper, we focus on feed-forward neural networks equipped with ReLU activation functions. A feed-forward network N consists of L layers, where each layer alternates between a linear transformation and a ReLU activation. For the l -th layer, we denote the pre-activation and post-activation values as $z^{(l)}(x)$ and $\hat{z}^{(l)}(x)$, respectively. These are computed as follows: $z^{(l)}(x) = W^{(l)}z^{(l-1)}(x) + b^{(l)}$, $\hat{z}^{(l)}(x) = \text{ReLU}(z^{(l)}(x))$, where $W^{(l)}$ and $b^{(l)}$ represent the weight matrix and bias vector of the l -th layer, respectively.

Let d_l denote the number of neurons in the l -th layer, and let $N_{i,l}$ refer to the i -th neuron in that layer. The pre-activation and post-activation values of $N_{i,l}$ for a given input x are $z_i^{(l)}(x)$ and $\hat{z}_i^{(l)}(x)$, respectively. The network as a whole can be viewed as a function $F^{<N>} : \mathbb{R}^{d_0} \rightarrow \mathbb{R}^{d_L}$, where $F^{<N>}(x) = z^{(L)}(x)$ represents the output of the final layer. For the i -th neuron in the last layer, its output is $F_i^{<N>}(x) = z_i^{(L)}(x)$. When the context is clear, we omit N for simplicity and refer to the network as F . In multi-class classification tasks with C classes, the network predicts the class $c \in C$ for a given input x if the output $F_c(x)$ of the c -th neuron in the L -th layer is the largest among all outputs.

2.2 Adversarial Attacks and Neural Networks Verification Problem

Given a neural network F and a reference point x , adversarial attacks aim to search for a point x' that is geometrically close to the reference point x such that x' and x belong to different classes. Here, we use the canonical specification, that is, we want to search in the local neighborhoods (L_∞ norm balls) of x , formally denoted as $B(x, \epsilon) := \{x' \mid \|x - x'\|_\infty \leq \epsilon\}$, where ϵ is the radius. For certain ϵ , given we know x belongs to class j , we say an adversarial point is found if:

$$\exists x' \in B(x, \epsilon) \quad \exists i \in C \quad F_i(x') - F_j(x') > 0 \quad (1)$$

In practice, the change from the original data x to adversarial data x' should be imperceptible, so they are more likely to be recognized as the same class/label from a human perspective. There are also metrics other than the L_∞ norm to represent the "similarity" between x and x' , such as the L_0 and L_2 norms [Xu et al. 2020]. However, almost all of them fall into the local neighborhood specification paradigm. This is different from the NAP specification, as we will discuss later.

Neural networks are vulnerable to adversarial attacks, where even imperceptible changes can alter predictions significantly. This underscores the critical need for neural network verification, which can be viewed as highlighting safe regions that excludes adversarial regions. Solving the verification problem involves formally proving the absence of adversarial points in $B(x, \epsilon)$. Formally, the verification problem seeks to prove:

$$\forall x' \in B(x, \epsilon) \quad \forall i \neq j \quad F_j(x') - F_i(x') > 0 \quad (2)$$

For a simpler presentation, we assume that $F(x)$ is a binary classifier. For any given specification $B(x, \epsilon)$, $F(x) \geq 0$ indicates that the model is verified; otherwise, we can find an adversarial example. Solving such a verification problem is known to be NP-hard [Katz et al. 2017b], and achieving scalability in verification remains an ongoing challenge.

2.3 Neuron Abstractions and Neural Activation Patterns

To better discuss NAP specification and robustness verification, we first introduce the relevant concepts of neuron abstractions, neuron abstraction functions, and neural activation patterns.

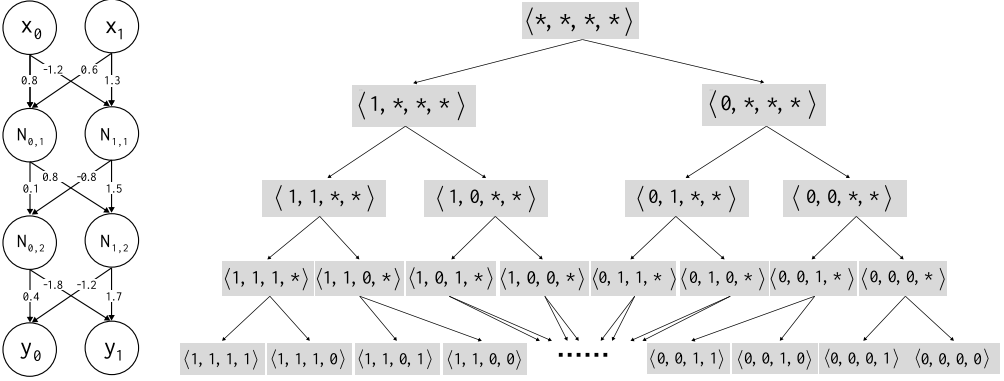
Neuron Abstractions. For a neural network N , an internal neuron $N_{i,l}$ (where $0 \leq i \leq d_l$ and $1 \leq l \leq L-1$) can have its post-activation value $\hat{z}_i^{(l)}(x)$ abstracted into finite states. This abstraction is a mapping from \mathbb{R} to a set $\mathbb{S} = \{s_1, s_2, \dots, s_n\}$, representing neuron states. A simple binary abstraction for ReLU activation defines two states: $s_0 := 0$ (deactivation) and $s_1 := (0, \infty)$ (activation). Further, these states can be abstracted into a unary state $s_* = [0, \infty)$, covering the entire range of post-activation. This leads to a partial order: $s_* \leq s_0$ and $s_* \leq s_1$, where s_0 and s_1 refine s_* . For simplicity, we use $\mathbf{0}, \mathbf{1}, *$ to represent these states. Our specification learning approach applies to any activation function definable within the abstraction domain, though this study focuses on ReLU.

Definition 2.1 (Neuron Abstraction Function). Given a neural network N and the abstraction state set \mathbb{S} . A neuron abstraction function is a mapping $\mathcal{A} : N \rightarrow \mathbb{S}$. Formally, for an arbitrary neuron $N_{i,l}$, the function abstracts $N_{i,l}$ to some state $s_k \in \mathbb{S}$, i.e., $\mathcal{A}(N_{i,l}) = s_k$.

The above characterization of neuron abstraction does not instruct us on how to perform binary abstraction in the absence of neuron values. Therefore, we introduce two types of \mathcal{A} : unary $\hat{\mathcal{A}}$ and binary $\check{\mathcal{A}}$, both of which take a single input x as a parameter, omitting it when the context is clear.

The unary $\hat{\mathcal{A}}$ function. $\hat{\mathcal{A}}$ always maps any input to the coarsest state $*$. Formally:

$$\hat{\mathcal{A}}(N_{i,l}, x) = * \quad (3)$$



(a) A simple 2x2 fully connected neural network. each neuron is either 1 or 0. From the root, the tree is spanned by abstracting each neuron in an order of $N_{0,1}, N_{1,1}, N_{0,2}, N_{1,2}$. Setting a different order will create a different tree of NAPs.

Fig. 2. A simple 2x2 fully connected neural network and a subset of its NAP in a binary tree structure.

The binary $\ddot{\mathcal{A}}$ function. When an input x is passed through an internal neuron $N_{i,l}$, we can easily determine the binary abstraction state of $N_{i,l}$ based on its post-activation value $\hat{z}_i^{(l)}(x)$. This motivates us to define the binary abstraction function as follows:

$$\ddot{\mathcal{A}}(N_{i,l}, x) = \begin{cases} 0 & \text{if } \hat{z}_i^{(l)}(x) = 0 \\ 1 & \text{if } \hat{z}_i^{(l)}(x) > 0 \end{cases} \quad (4)$$

Definition 2.2 (Neural Activation Pattern). Given a neural network N , an input x , and neuron abstraction functions $\ddot{\mathcal{A}}$ and $\dot{\mathcal{A}}$, a neural activation pattern (NAP) P is a tuple representing the abstraction state of all neurons in N . Formally, $P := \langle \mathcal{A}(N_{i,l}, x) \mid N_{i,l} \in N \rangle$, where \mathcal{A} is either $\ddot{\mathcal{A}}$ or $\dot{\mathcal{A}}$, chosen for each neuron. We also denote P as $\mathcal{A}(N, x)$. The abstraction state of neuron $N_{i,l}$ is represented as $P_{i,l}$, specifically $P_{i,l} = \mathcal{A}(N_{i,l}, x)$. When representing a refined activation pattern triggered by x where $\ddot{\mathcal{A}}$ is applied to each neuron, it is expressed as $\ddot{\mathcal{A}}(N, x)$.

We denote the power set of NAPs in N as \mathcal{P} . The number of all possible NAPs in N scales exponentially as the number of neurons increases. For such a large set, if we aim to find the minimal NAP – the central problem in this work, we first have to establish an order so that NAPs can be compared. To this end, we define the following partial order:

Definition 2.3 (Partially ordered NAP). For any given two NAPs $P, P' \in \mathcal{P}$, we say P' subsumes P if, for each neuron $N_{i,l}$, its state in P is an abstraction of that in P' . Formally, this can be defined as:

$$P' \leq P \iff P'_{i,l} \leq P_{i,l} \quad \forall N_{i,l} \in N \quad (5)$$

Moreover, two NAPs P, P' are equivalent if $P \leq P'$ and $P' \leq P$.

To give a concrete example, Figure 2b depicts a subset of all possible NAPs of a simple neural network consisting of 2 hidden layers and 4 neurons, as presented in Figure 2a. It is noteworthy that a subset of the NAP family \mathcal{P} can form a complete binary tree based on the order of abstraction in neurons. For example, using the order $N_{0,1}, N_{1,1}, N_{0,2}, N_{1,2}$ creates a specific tree of NAPs; different

orders will yield different trees. The root of this tree is the coarsest NAP, $\langle *, *, *, * \rangle$. Increasing the tree’s depth means that $\tilde{\mathcal{A}}$ applies to more neurons, and at the leaf nodes, all neurons are abstracted by $\tilde{\mathcal{A}}$. The leaf nodes represent the most refined NAPs, totaling $2^{|N|}$. Additionally, each parent node subsumes its child, meaning a leaf node will always be subsumed by its ancestors along the path. For example, we have the relationship:

$$\langle *, *, *, * \rangle \preceq \langle 1, 0, *, * \rangle \preceq \langle 1, 0, 1, * \rangle \preceq \langle 1, 0, 1, 0 \rangle.$$

However, children under the same parent are not comparable, as seen in $\langle 1, 0, *, * \rangle \not\preceq \langle 1, 1, *, * \rangle$. This occurs because these NAPs reside on different branches formed by splitting certain ReLUs.

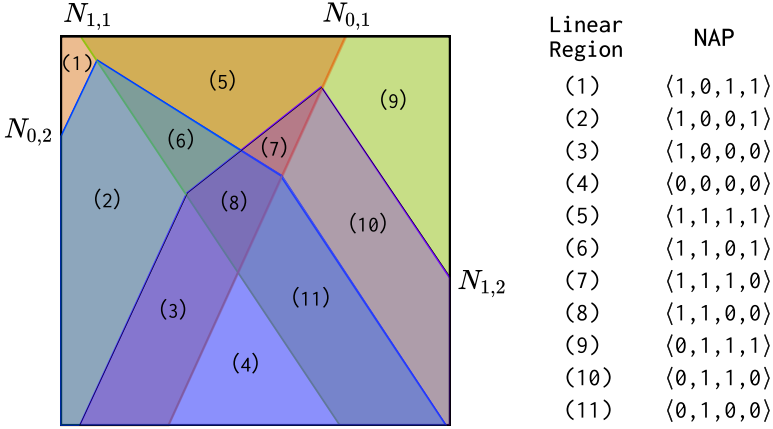


Fig. 3. Linear regions are shattered by the simple 2X2 neural network. Each linear region corresponds to a most refined NAP, but not necessarily vice versa. More abstracted NAPs are formed by ignoring lines/hyperplanes created by neurons.

Regions Outlined by NAPs. A key requirement for verification specifications is their ability to represent specific regions within the input space. Canonical local neighbor specifications define L_∞ norm balls using explicit formulas, such as $B(x, \epsilon) := \{x' \mid \|x - x'\|_\infty \leq \epsilon\}$. In contrast, NAP specifications implicitly outline certain regions in the input space. We define the regions specified by P as R_P , which represents the set of inputs whose activation patterns subsumed by the given NAP P . Formally, $R_P := \{x \mid P \preceq \tilde{\mathcal{A}}(N, x)\}$. For instance, Figure 3 illustrates the NAP family of the simple neural network shown in Figure 2a. These NAPs correspond to regions bounded by hyperplanes created by neurons, with the most refined NAPs representing individual linear regions from (1) to (11). For example, linear region (9) corresponds to $\langle 0, 1, 1, 1 \rangle$. The coarsest state $*$ abstracts the binary states 0 and 1 , allowing a NAP with more $*$ to cover a larger, potentially concave region in the input space. For instance, the NAP $\langle *, *, 1, * \rangle$ corresponds to the union of linear regions (1), (5), (7), (9), and (10). Notably, the number of linear regions is less than the size of the NAP family, as reported in [Geng et al. 2022; Hanin and Rolnick 2019a,b].

2.4 NAP Specifications for Robustness Verification

The previously introduced NAP definition primarily serves as a conceptual tool. To function as a specification for robustness verification, the regions outlined by NAPs (R_P) should cover a significant amount of data from a specific class. We demonstrate how to achieve this using the $\tilde{\mathcal{A}}$ function.

The statistical $\tilde{\mathcal{A}}$ function. The binary $\tilde{\mathcal{A}}$ function is limited to processing a single input and encounters challenges when multiple inputs are involved, as two distinct inputs may lead to conflicting abstraction states for a neuron; for instance, a neuron may be deactivated for input x_1 but activated for another input x_2 . This can be problematic when attempting to learn a general NAP for an entire class of inputs. To address this issue, we approach it statistically by introducing the $\tilde{\mathcal{A}}$ function, defined as follows:

$$\tilde{\mathcal{A}}(N_{i,l}, X) = \begin{cases} 0 & \text{if } \frac{|\{x_j | \tilde{\mathcal{A}}(N_{i,l}, x_j)=0, x_j \in X\}|}{|X|} \geq \delta \\ 1 & \text{if } \frac{|\{x_j | \tilde{\mathcal{A}}(N_{i,l}, x_j)=1, x_j \in X\}|}{|X|} \geq \delta \\ * & \text{otherwise} \end{cases} \quad (6)$$

where δ is a real number from $[0, 1]$, and X represents a set of inputs, i.e., $X := \{x_1, x_2, \dots, x_n\}$. Since datasets often contain noisy data or challenging instances that the model cannot predict accurately, we introduce the parameter δ to accommodate standard classification settings in which Type I and Type II errors are non-negligible. Intuitively, the introduction of δ allows multiple inputs x_1, \dots, x_n to vote on a neuron’s state. For instance, when δ is set to 0.99, then 99% or more of the inputs must agree that a neuron is activated for the neuron to be in the 1 state. It is worth mentioning that the statistical $\tilde{\mathcal{A}}$ function is equivalent to the method described in Geng et al. [2023].

Definition 2.4 (Class NAP). In a classification task with the class set C , for any class $c \in C$, a class NAP P^c is a NAP comprising abstract states outputted by an abstraction function given X_c , where X_c denotes the set of inputs belonging to class c . Formally, $P^c := \langle \mathcal{A}(N_{i,l}, X_c) \mid N_{i,l} \in N \rangle$, where \mathcal{A} is either $\tilde{\mathcal{A}}$ or \mathcal{A} , chosen for each neuron. The power set of P^c is denoted as \mathcal{P}^c .

Robustness verification involves proving that no adversarial examples exist in the local neighborhood of a reference point x . For NAP specifications, this translates to showing that no adversarial examples exist in class NAP P^c ; in other words, inputs exhibiting P^c must be classified as c . Geng et al. [2023] argues that class NAPs must meet several key requirements to qualify as NAP specifications, and finding such NAPs effectively verifies the underlying robustness problem. We formalize these requirements into the following properties:

The non-ambiguity property. Since we want class NAPs to serve as certificates for a certain class, they must be distinct from each other. Otherwise, there could exist an input that exhibits two class NAPs, which leads to conflicting predictions. Formally, we aim to verify the following:

$$\forall x \quad \forall c_1, c_2 \in C \text{ s.t. } c_1 \neq c_2 \quad P^{c_1} \leq \tilde{\mathcal{A}}(N, x) \implies P^{c_2} \not\leq \tilde{\mathcal{A}}(N, x) \quad (7)$$

From a geometric perspective, there must be no overlaps between class NAPs. In other words, it is also equivalent to verifying:

$$\forall c_1, c_2 \in C \text{ s.t. } c_1 \neq c_2 \quad R_{P^{c_1}} \cap R_{P^{c_2}} = \emptyset$$

The NAP robustness property. To serve as NAP specifications, class NAPs P^c ensure that if an input exhibits it, i.e., $P \leq \tilde{\mathcal{A}}(N, x)$, the input must be predicted as the corresponding class c . Formally, we have:

$$\forall x \in R_{P^c} \quad \forall k \in C \text{ s.t. } k \neq c \quad F_c(x) - F_k(x) > 0 \quad (8)$$

in which

$$R_{P^c} = \{x \mid P^c \leq \tilde{\mathcal{A}}(N, x)\} \quad (9)$$

The NAP-augmented robustness property. Rather than relying exclusively on class NAPs as specifications, local neighbors can also be used in combination for verification. This hybrid approach offers several advantages: 1) It narrows the scope of verifiable regions when class NAPs alone cannot satisfy the NAP robustness property; 2) NAP constraints essentially lock ReLU states, thereby refining the search space for verification tools; 3) It emphasizes verifying valid test inputs, while still covering broader and more flexible verifiable regions than those defined by L_∞ norm ball specifications alone. Formally, this property can be expressed as:

$$\forall x' \in B(x, \epsilon) \bigcap R_{P^c} \quad \forall k \in C \text{ s.t. } k \neq c \quad F_c(x) - F_k(x) > 0 \quad (10)$$

in which

$$B(x, \epsilon) = \{x' \mid \|x - x'\|_\infty \leq \epsilon\} \quad R_{P^c} = \{x' \mid P^c \preceq \tilde{\mathcal{A}}(N, x')\} \quad (11)$$

To summarize, we state that a class NAP can serve as a NAP specification if it satisfies either the NAP robustness property or the NAP-augmented robustness property. Clearly, the former property is stronger, and it is possible that we can't find a class NAP P^c in \mathcal{P}^c to satisfy this property. Fortunately, we can always find NAPs that satisfy the latter property by narrowing the verifiable region with additional L_∞ norm ball specifications.

3 THE MINIMAL NAP SPECIFICATION PROBLEM

In this section, we formulate the problem of learning minimal NAP specifications and present both a deterministic and statistical approach to address it. As our methods involve interactions with verification tools, we first introduce the relevant notations.

3.1 Problem Formulation

Let (\mathcal{P}^c, \preceq) be a partially ordered set corresponding to a family of class NAPs regarding some class $c \in C$. For simplicity, we omit the superscript c and refer to class NAPs simply as NAPs when the context is clear. We assume access to a verification tool, $\mathcal{V} : \mathcal{P} \rightarrow \{0, 1\}$, which maps a class NAP $P \in \mathcal{P}$ to a binary set. Here, $\mathcal{V}(P) = 1$ denotes a successful verification of the underlying robustness query, while 0 indicates the presence of an adversarial example. From an alternative perspective, $\mathcal{V}(P) = 1$ also signifies that P is a NAP specification, i.e., it satisfies NAP(-augmented) robustness properties; whereas $\mathcal{V}(P) = 0$ implies the opposite.

It is not hard to see that \mathcal{V} is monotone with respect to the NAP family (\mathcal{P}, \preceq) . Given $P' \preceq P$ and $\mathcal{V}(P') = 1$, it follows that $\mathcal{V}(P) = 1$. However, given $P' \preceq P$ and $\mathcal{V}(P) = 1$, we cannot determine $\mathcal{V}(P')$. In other words, refining a NAP (by increasing the number of neurons abstracted to **0** or **1**) can only enhance the likelihood of successful verification of the underlying robustness query.

Definition 3.1 (The minimal NAP specification problem). Given a family of NAPs \mathcal{P} and a verification tool \mathcal{V} , the minimal NAP specification problem is to find a NAP P such that:

$$\forall P' \preceq P, P' \neq P \implies \mathcal{V}(P') = 0$$

That is, when P is minimal, any NAP P' that is strictly coarser than P will result in $\mathcal{V}(P') = 0$. The size of P , denoted by $|P|$ or s , represents the number of neurons abstracted to **0** or **1**, i.e., $|\{N_{i,l} \mid P_{i,l} = \mathbf{0} \text{ or } \mathbf{1}\}|$.

It is important to note that "minimal" refers to the level of abstraction, not the size of the NAP. Since (\mathcal{P}^c, \preceq) is a partially ordered set, multiple minimal NAP specifications may exist, rather than a single global minimum. In such cases, selecting any one of the minimal NAPs is sufficient. However, it is possible that even the most refined NAPs cannot verify the robustness query, in which case no minimal NAP specification exists. Given the computational cost of using verification

tools, we are particularly interested in methods that efficiently find a minimal NAP specification, minimizing the number of calls to \mathcal{V} .

3.2 Conservative Bottom Up Approach

We introduce COARSEN, a method that starts with the most refined NAP and gradually coarsens it to learn minimal NAP specifications. Before proceeding, we define the relevant notations.

Given a class input X_c , the coarsest NAP is defined as the one that uses $\tilde{\mathcal{A}}$ to abstract each neuron in N , denoted as $\dot{P} := \langle \tilde{\mathcal{A}}(N_{i,l}, X_c) \mid N_{i,l} \in N \rangle$. This NAP is the smallest possible in size, with $|\dot{P}| = 0$. Conversely, the most refined NAP applies $\tilde{\mathcal{A}}$ to abstract each neuron, denoted as $\bar{P} := \langle \tilde{\mathcal{A}}(N_{i,l}, X_c) \mid N_{i,l} \in N \rangle$ or $\tilde{\mathcal{A}}(N)$. This NAP is the largest in size, with $|\bar{P}| \leq |N|$. Clearly, we have $\dot{P} \leq \bar{P}$.

To refine any NAP P through a specific neuron $N_{i,l}$, we apply the $\tilde{\mathcal{A}}$ function, denoting this refinement as $\tilde{\Delta}(N_{i,l})$. This action may either increase or leave $|P|$ unchanged. Conversely, we denote the coarsen action as $\dot{\Delta}(N_{i,l})$, which will either decrease or leave $|P|$ unchanged.

The COARSEN approach starts by verifying if the most refined NAP \bar{P} successfully passes verification. For each neuron, we attempt to coarsen it using $\dot{\Delta}$. If the resulting NAP no longer verifies the query, we revert to refining it back using $\tilde{\Delta}$; otherwise, we retain the coarsened NAP. The procedure is detailed in Algorithm 1, which may require up to $|N|$ calls to \mathcal{V} in the worst case, as shown in Theorem 3.2. Please refer to the proof in Appendix D.

Algorithm 1: COARSEN

Input: The neural network N

Output: A minimal NAP specification P

```

1 Function Coarsen( $N$ )
2    $P \leftarrow \tilde{\mathcal{A}}(N)$ 
3   if  $\mathcal{V}(P) == 0$  then
4     | return None; /* Return None if the most refined NAP fails verification */
5   else
6     | for  $N_{i,l}$  in  $N$  do
7       |    $P \leftarrow \dot{\Delta}(N_{i,l})$ ; /* Try to coarsen(abstract) this neuron using  $\dot{\Delta}$  */
8       |   if  $\mathcal{V}(P) == 0$  then
9         |     |  $P \leftarrow \tilde{\Delta}(N_{i,l})$ ; /* Refine the neuron back if the verification fails */
10      |   return  $P$ ;

```

Theorem 3.2. *The algorithm COARSEN returns a minimal NAP specification with $O(|N|)$ calls to \mathcal{V} .*

3.3 Statistical Coarsen Approach

The COARSEN algorithm initiates with the most refined NAP and progressively coarsens each neuron until verification fails. Enhancing the algorithm’s performance is possible by coarsening multiple neurons during each iteration. However, a fundamental question emerges: How do we determine which *set* of neurons to coarsen in each round?

We present STOCHCOARSEN to answer this question. In this approach, we assume that each neuron is independent of the others and select neurons to coarsen in a statistical manner. Specifically, in each iteration, we randomly coarsen a subset of refined neurons in the current NAP simultaneously to see if the new NAP can pass verification. We repeat this process until the NAP size reaches s . This method can be regarded as optimistic bottom up. Algorithm 2 provides the pseudocode for STOCHCOARSEN.

It’s important to note that the stochastic manner of this algorithm faces the challenge of sample efficiency. For instance, if a minimal NAP specification P of size s is identified after one iteration, the probability of selecting the exact s essential neurons in P is θ^s . Consequently, if we set θ as a constant, the expected number of samples required to find the NAP becomes $(\frac{1}{\theta})^s$.

STOCHCOARSEN allows us to narrow down the estimated essential neurons by an expected factor of θ once a valid NAP is learned. Thus, the expected number of samples and iterations are inversely related, with their product equating to the total calls to \mathcal{V} . By setting $\theta = e^{-\frac{1}{s}}$, we can achieve polynomial expected samples in s while minimizing the total number of calls to \mathcal{V} , as proven in Theorem 3.3. The proof is detailed in Appendix E.

Algorithm 2: STOCHCOARSEN

Input: The neural network N , the probability θ , and the size s
Output: A minimal NAP specification P

```

1 Function StochCoarsen(mand_neurons,  $\theta$ ,  $s$ )
2    $P \leftarrow \tilde{\mathcal{A}}(N)$ ; mand_neurons  $\leftarrow N$ 
3   if  $\mathcal{V}(P) == 0$  then
4     return None /* Return None if the most refined NAP fails verification */
5   else
6     while  $|P| > s$  do
7        $P \leftarrow \text{Sample\_NAPs}(\text{mand\_neurons}, \theta)$ 
8       if  $\mathcal{V}(P) == 1$  then
9         found_neurons  $\leftarrow \emptyset$ 
10        for  $N_{i,l}$  in  $N$  do
11          if  $P_{i,l} == \tilde{\mathcal{A}}(N_{i,l})$  then
12            found_neurons  $\leftarrow \text{found\_neurons} \cup \{N_{i,l}\}$ 
13          mand_neurons  $\leftarrow \text{found\_neurons}$  /* Reduce search space */
14        else
15           $P \leftarrow \text{Sample\_Naps}(\text{mand\_neurons}, \theta)$  /* Sample a new NAP */
16      return  $P$  /* Return the minimal NAP of size  $s$  */

```

Theorem 3.3. *With probability $\theta = e^{-\frac{1}{s}}$, STOCHCOARSEN learns a minimal NAP specification with $O(s \log |N|)$ calls to \mathcal{V} .*

Setting the sample probability θ . Setting s poses a challenge in practice, as we assume that s is always provided in STOCHCOARSEN. However, this can be addressed by dynamically updating θ based on the result of $\mathcal{V}(P)$ [Liang et al. 2011]. With θ from theorem 3.3, STOCHCOARSEN finds a NAP specification with probability $(e^{-1/s})^s = e^{-1}$. Thus, we aim to set θ such that the $Pr(\mathcal{V}(P) = 1) = e^{-1}$. Intuitively, if a sampled NAP P is a specification, we decrease θ so more neurons will be coarsened. Similarly, if P is not a specification, θ needs to be increased.

Given that $\theta \in [0, 1]$, we can parameterize it using the Sigmoid function $\sigma(\lambda) = (1 + e^{-\lambda})^{-1}$, where $\lambda \in (-\infty, \infty)$. Since $Pr(\mathcal{V}(P) = 1)$ depends on θ as well, we express it as a function of λ , $g(\lambda) = Pr(\mathcal{V}(P) = 1)$. Then, setting $Pr(\mathcal{V}(P) = 1) = e^{-1}$ can be achieved through the following minimization problem:

$$L(\lambda) = \frac{1}{2}(g(\lambda) - e^{-1/s})^2 \quad (12)$$

The loss function $L(\lambda)$ can be minimized by statistical learning using stochastic gradient descent. With a step size η , update λ using $\lambda \leftarrow \lambda - \eta \frac{dL}{d\lambda}$. Note that $\frac{dL}{d\lambda}$ can be expressed as:

$$\frac{dL}{d\lambda} = (g(\lambda) - e^{-1/s}) \frac{dg(\lambda)}{d\lambda} \quad (13)$$

Given $g(\lambda) = \Pr(\mathcal{V}(P) = 1)$, we can replace $g(\lambda)$ with $\mathcal{V}(P)$ for stochastic gradient update. Additionally, since $\frac{dg(\lambda)}{d\lambda} > 0$, we simply ignore it as its multiplication effect can be represented by η . Therefore, the final update rule is given by:

$$\lambda \leftarrow \lambda - \eta(\mathcal{V}(P) - e^{-1}) \quad (14)$$

4 OPTIMISTIC APPROACH

While COARSEN and STOCHCOARSEN effectively identify minimal NAP specifications with correctness guarantees, their practicality is limited by the extensive runtime required to perform a large number of expensive verification calls. This limitation makes them less suitable for time-critical applications or large-scale neural networks. To address these challenges, we propose a optimistic approach for efficiently initializing NAP specifications. This approach significantly reduces the number of subsequent verification calls and provide a reliable upper bound on the size of the minimal NAP specification, improving both efficiency and scalability. The approach focuses on the concept of essential neurons, key to understanding the minimal NAP specification problem.

Definition 4.1 (Essential neuron). A neuron $N_{i,l} \in N$ is considered essential if it cannot be coarsened to $*$ in any minimal NAP specification. We denote the set of all essential neurons as E , defined by:

$$E = \{N_{i,l} \mid P_{i,l} \in \{0, 1\}, P \text{ is minimal}\}$$

Note that E is the union of the set of essential neurons from all minimal NAP specifications. It follows that $|E| \geq s$, where s denotes the size of the largest minimal NAP specification.

The minimal NAP specification problem can be solved trivially if we gain access to E . Thus, our optimistic approach is designed to determine essential neurons and estimate E . To better understand our approach, we first discuss the properties of essential neurons. Recall that verifying a robustness query given a NAP specification P is equivalent to showing that $F(x) \geq 0$ for input x in region R_P . Thus, the necessary conditions of a essential neuron $N_{i,l}$ can be written as follows:

- (1) If $N_{i,l}$ is in state $\mathbf{0}$, it implies when $\hat{z}_i^{(l)}(x) = 0, F(x) \geq 0$. In addition, $\exists x$ s.t. $\hat{z}_i^{(l)}(x) > 0, F(x) < 0$.
- (2) If $N_{i,l}$ is in state $\mathbf{1}$, it implies $\forall x$ s.t. $\hat{z}_i^{(l)}(x) > 0, F(x) \geq 0$. In addition, when $\hat{z}_i^{(l)}(x) = 0, F(x) < 0$.

As for non-essential neurons in P , since they can be coarsened to $*$, it implies $F(x) \geq 0$ regardless of the value of $\hat{z}_i^{(l)}(x)$. Formally, this can be written as: If $N_{i,l}$ is in state $\mathbf{0}$ or $\mathbf{1}$, it implies that $\forall x, F(x) \geq 0$. In the COARSEN algorithm, we rely on interaction with the verification tool \mathcal{V} to identify essential neurons. Since calls to \mathcal{V} are typically computationally expensive, it would be advantageous to estimate E in a more cost-effective manner. This motivates us to study the following optimistic approach.

We introduce OPTADVPRUNE to identify essential neurons. Intuitively, it attempts to show a neuron $N_{i,l}$ is essential by actively falsifying NAP candidates with adversarial examples. When an adversarial example x' is found, it immediately indicates that the NAP $\tilde{\mathcal{A}}(N, x')$ fails the verification, i.e., $\mathcal{V}(\tilde{\mathcal{A}}(N, x')) = 0$. Moreover, it also implies that any NAP subsumed by $\tilde{\mathcal{A}}(N, x')$ fails verification. For instance, suppose an adversarial example x' is found for a simple one-layer four-neuron neural network and $\tilde{\mathcal{A}}(N, x')$ is $\langle \mathbf{1}, \mathbf{0}, \mathbf{1}, \mathbf{0} \rangle$. We can infer that NAPs like $\langle \mathbf{1}, \mathbf{0}, \mathbf{1}, * \rangle$, $\langle \mathbf{1}, \mathbf{0}, *, * \rangle$, $\langle \mathbf{1}, *, *, \mathbf{0} \rangle$, and $\langle \mathbf{1}, \mathbf{0}, *, \mathbf{0} \rangle$ fail the verification. This information is particularly useful when determining if a neuron is essential. For example, if we know that NAP $P := \langle \mathbf{1}, \mathbf{0}, *, \mathbf{1} \rangle$ is a

Algorithm 3: OPTADVPRUNE**Input:** The neural network N , the input dataset X **Output:** A collection of essential neurons

```

1 Function OptAdvPrune( $N, X$ )
2    $Mand \leftarrow \emptyset$ ;  $P \leftarrow \tilde{\mathcal{A}}(N)$ 
3   for  $x_j$  in  $X$  do
4      $x'_j \leftarrow \text{Adversarial\_Attack}(x_j)$ 
5     for  $N_{i,l}$  in  $N$  do
6       if  $P_{i,l} \in \{0, 1\}$  and  $\tilde{\mathcal{A}}(N_{i,l}, x'_j) \oplus P_{i,l}$  then
7          $Mand \leftarrow Mand \cup \{N_{i,l}\}$            /* Create essential neurons for  $x'_j$  */
8   return  $Mand$ 

```

specification, i.e., $\mathcal{V}(P) = 1$, then we can easily deduce that the fourth neuron $N_{4,1}$ is essential. This is because that coarsening the fourth neuron would expand P to $\langle 1, 0, *, * \rangle$, which would include the adversarial example x' and thus fail the verification, as illustrated in Figure 4a. It is evident that the neuron where P and $\tilde{\mathcal{A}}(N, x')$ disagrees must be essential.

However, when the two NAPs disagree on multiple neurons, things become a little bit different. Suppose the NAP specification P is $\langle 1, 1, *, 1 \rangle$, i.e., $\mathcal{V}(\langle 1, 1, *, 1 \rangle) = 1$. We know $\mathcal{V}(\langle 1, 0, *, 0 \rangle) = 0$ by the adversarial example x' . In this case, if we coarsen the second and fourth neurons, $N_{2,1}$ and $N_{4,1}$, the NAP specification will expand to $\langle 1, *, *, * \rangle$, which will cover the $\langle 1, 0, *, 0 \rangle$, thus failing the verification. In this case, $N_{2,1}$ and $N_{4,1}$ could both be essential neurons or either one of them is essential, as illustrated in Figures 4b, 4c, 4d. So, we simply let $\{N_{2,1}, N_{4,1}\}$ be the upper bound of essential neurons (learned from x'). Formally, given a NAP P , we say a neuron $N_{i,l}$ is in the upper bound of essential neurons E if satisfies the following condition:

- (1) $N_{i,l}$ must be in the binary states, i.e., $P_{i,l} \in \{0, 1\}$
- (2) There exists x' such that $\tilde{\mathcal{A}}(N_{i,l}, x')$ XORs with $P_{i,l}$, i.e., $\exists x'$ such that $\tilde{\mathcal{A}}(N_{i,l}, x') \oplus P_{i,l} = 1$

The field of adversarial attacks provides a diverse set of computationally efficient methods, enabling access to numerous adversarial examples. In this study, we use a collection of different

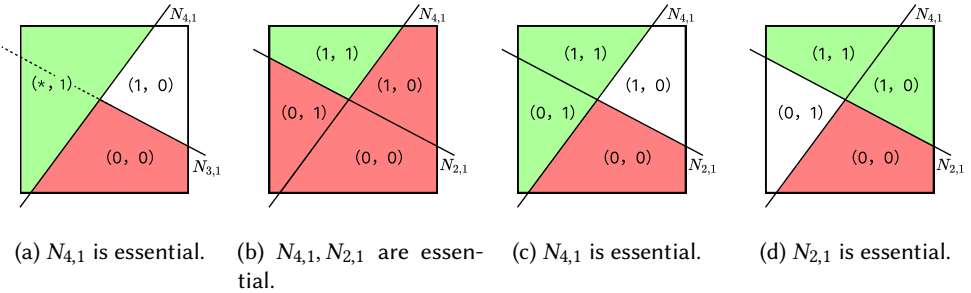


Fig. 4. Geometric interpretation of NAPs on essential neurons. The first subfigure represents the case when the two NAPs disagree on $N_{4,1}$. The other three subfigures represent the three cases when the two NAPs disagree on $N_{4,1}, N_{2,1}$. Regions colored green pass verification, whereas red indicates an adversarial example exists. Here, we omit states for $N_{1,1}, N_{3,1}$ in those NAPs for simplicity.

attacks, including the Projected Gradient Descent (PGD) attack [Madry et al. 2018] and the Carlini-Wagner (CW) attack [Carlini and Wagner 2017]. By computing the upper bound of essential neurons for each adversarial example and taking their union, we efficiently estimate the overall upper bound, as shown in Algorithm 3.

5 VOLUME ESTIMATION OF R_P

Conceptually, NAP specifications typically correspond to significantly larger input regions compared to local neighbourhood specifications. This serves as the primary motivation for utilizing NAPs as specifications. However, previous work lacks sufficient justification or evidence to support this claim. In this section, we propose a simple method for approximating the volume of R_P , i.e., the region corresponding to a NAP P . This allows us to: 1) quantify the size difference between R_P and L_∞ ball specifications; 2) gain insights into the volumetric change from the most refined NAP specification to the minimal NAP specification.

Computing the exact volume of R_P is at least NP-hard, as determining the exact volume of a polygon is known to be NP-hard [Dyer and Frieze 1988]. Moreover, computing the exact volume of R_P can be even more challenging due to its potential concavity. To this end, our method estimates the volume of R_P by efficient computation of an orthotope that closely aligns with R_P , as illustrated in Figure 5. We briefly describe it as follows:

Finding an anchor point. The first step is to find an anchor point to serve as the center of the orthotope. Ideally, this anchor point should be positioned close to the center of R_P to ensure a significant overlap between the orthotope and R_P . However, computing the actual center of R_P is costly. Thus, we look for a pseudo-center from the training set X that resides in R_P . This pseudo-center can be computed by finding the point that uses the smallest L_∞ ball to cover other data points, solved as the following optimization problem:

$$c_{\text{pseudo}} = \arg \min_{x \in R_P} \max_{x' \in R_P} \|x - x'\|_\infty$$

where $R_P = \{x \mid \mathcal{A}(N, x) \leq P, x \in X\}$. When $|X|$ is small, c_{pseudo} can be computed directly; for larger $|X|$, a statistical computation strategy is required.

Constructing the orthotope. Once the pseudo-center c_{pseudo} is determined, we want to create an orthotope around c_{pseudo} to closely align with R_P . The orthotope is constructed by determining pairs of upper and lower bounds $U^{(i)}$ and $L^{(i)}$ for each dimension i . Specifically, $U^{(i)}$ and $L^{(i)}$ are computed through expansion in two opposite directions from c_{pseudo} along dimension i until they extend beyond R_P . This expansion can be expressed as:

$$\max_{U^{(i)}} \{x' \in R_P \mid x' := c_{\text{pseudo}} + U^{(i)}\} ; \max_{L^{(i)}} \{x' \in R_P \mid x' := c_{\text{pseudo}} - L^{(i)}\}$$

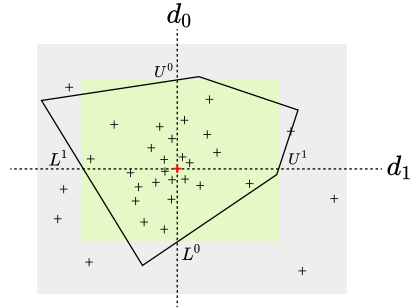


Fig. 5. Volume Estimation of R_P using an orthotope in a 2-dimensional case. The gray rectangle represents the input space, with the training set depicted by a collection of data points $+$. The polygon corresponds to some NAP P . Initially, we identify an anchor point, denoted by $+$. Then, we construct the orthotope, represented by the green rectangle, by extending upper and lower bounds starting from the anchor point until it extends beyond P .

Here, $U^{(i)}$ and $L^{(i)}$ represent the upper and lower bounds in dimension i respectively, originating from c_{pseudo} . These bounds can be efficiently calculated with binary search.

The choice of the archer point is crucial in our approach. If it is located at a corner of R_p , the volume calculation will be highly biased. This can pose a problem when we seek to understand the volumetric change from the most refined NAP specification to the minimal NAP specification. Additionally, using the orthotope as an estimator provides convenience in understanding the volumetric change simply by examining differences in each input dimension.

6 EVALUATION

In this section, we conduct a comprehensive evaluation of our algorithms for learning minimal NAP specifications across a range of benchmarks, from decision-critical tasks in cancer diagnosis to state-of-the-art image classification models. To illustrate the effectiveness of our approaches, we chose the method proposed in [Geng et al. 2023] as the baseline, denoted as the $\tilde{\mathcal{A}}$ function.

Experiment Setup. All experiments in this section were conducted on an Ubuntu 20.04 LTS machine with 172 GB of RAM and an Intel(R) Xeon(R) Silver Processor. For verification, we utilized Marabou [Katz et al. 2019], a dedicated state-of-the-art neural network verifier. We set a timeout of 5 minutes for each query call to the verification tool. If the timeout is exceeded, the current neuron is retained in the minimal NAP specification even if its status cannot be determined.

6.1 The Wisconsin Breast Cancer Dataset with Binary Classifier

We conduct our first experiment using a four-layer neural network as a binary classifier, where each layer consists of 32 neurons. This classifier is trained on the Wisconsin Breast Cancer (WBC) dataset [Wolberg et al. 1995]. Our trained model achieves a test set accuracy of 95.61%. We calculate the most refined (baseline) NAP specifications \tilde{P}^0 and \tilde{P}^1 for labels 0 and 1 using the statistical abstraction function $\tilde{\mathcal{A}}$ with a confidence ratio of $\delta = 0.95$. The size of \tilde{P}^0 and \tilde{P}^1 are 102 and 93, respectively. In contrast, the sizes of the minimal NAP specifications learned by the COARSEN algorithm for labels 0 and 1 are significantly reduced to 31 and 32, respectively. It is worth mentioning that our optimistic approach provides a fairly accurate estimate of the essential neurons, despite computing rather loose upper bounds. To be more specific, OPTADVPRUNE compute 43 essential neurons for label 0, respectively, covering 25 out of the 31 essential neurons appearing in the minimal NAP specification for label 0 computed by COARSEN. For label 1, OPTADVPRUNE computes 39 essential neurons, covering 25 out of the 32 essential neurons appearing in the minimal NAP specification for label 1 computed by COARSEN.

The NAP specification learnt from OPTADVPRUNE are verified, showing it provides an optimistic upper bound to the size of minimal NAP with minimal verification calls yet finding neurons. We show its efficiency on small models. This sheds light to solving minimal NAP problem on large models when using Coarsen and STOCHCOARSEN are impossible given the current limit on verification engine. Regarding the statistical approaches, STOCHCOARSEN learnt NAP specifications of size 42 and 45 for label 0 and label 1 using only 47 and 41 calls to verification respectively.

Recall that one of the main motivations for learning the minimal NAP specifications is their potential to verify larger input regions compared to refined NAP specifications. To support this, we compute the percentile of unseen test data that can be verified using these NAPs. Test data, sampled from the input space, serve as a proxy to understand the verifiable bounds of different NAPs. We find that the most refined NAP specifications \tilde{P}^0 and \tilde{P}^1 cover 81.40% and 80.28% of test data for labels 0 and 1, respectively. In contrast, minimal NAP specifications cover 95.35% and 94.37% of test data for labels 0 and 1, respectively. To intuitively understand the change in verifiable regions R_p

Table 1. Overview of the size of learned minimal NAP specifications using various approaches on the WBC benchmark. The columns represent different labels, while each row corresponds to a different algorithm. $|P|$ denotes the size of the learned NAP, and $\#\mathcal{V}$ represents the number of calls to \mathcal{V} . The *train* and *test* columns report the percentile (%) of train and test data covered by P . We assess the effectiveness of NAP specifications in covering both training and test data, reporting the coverage percentage (%) along with the estimated change in volume, expressed as an order of magnitude (x) relative to a baseline normalized to 1.

	0					1				
	$ P $	$\#\mathcal{V}$	<i>train</i>	<i>test</i>	<i>vol.</i>	$ P $	$\#\mathcal{V}$	<i>train</i>	<i>test</i>	<i>vol.</i>
$\bar{\mathcal{A}}$ function (<i>baseline.</i>)	102	1	78.11	81.40	1	93	1	83.06	80.28	1
COARSEN	31	102	98.22	95.35	10^5	32	93	99.65	94.37	10^5
STOCHCOARSEN	42	47	94.69	92.34	10^3	45	41	94.15	91.52	10^2
OPTADVPRUNE	61	1	91.06	89.37	10^2	54	3	87.06	87.28	10^2

from refined to minimal NAP specifications, we compare their estimated volumes. The increase in estimated volume is substantial—on the order of 10^5 times larger for labels 0 and 1.

6.2 MNIST with Fully Connected Network

To show that our insights and approaches can be applied to more complicated datasets and networks, we conduct the second set of experiments using the `mnistfc_256x4` model [VNNCOMP 2021], a 4-layer fully connected network with 256 neurons per layer trained on the MNIST dataset. Due to space constraints, we present results for randomly selected classes 0, 1, and 4, with the remaining results provided in Appendix A.

We compute the most refined NAP specifications, \bar{P}^0 , \bar{P}^1 , and \bar{P}^4 , for these labels with a confidence level of $\delta = 0.99$. Their sizes are 751, 745, and 712, respectively, consistent with the baseline results from previous work [Geng et al. 2023]. In contrast, the minimal NAP specifications learned by the COARSEN algorithm for labels 0, 1, and 4 are significantly reduced to 480, 491, and 506, respectively, despite requiring over 700 calls. These specifications cover more than 98% of the training and test data, demonstrating a significant improvement over the baseline. For estimated volume, the volumetric changes can be on the order of magnitude of 10^9 larger. Notably, STOCHCOARSEN achieves comparable results with only around 30 calls, at the cost of approximately a 5% reduction in coverage on both training and test data compared to COARSEN. This highlights the potential of these learned minimal NAPs as robust specifications that generalize well to unseen data from the same distribution. In comparison, our empirical analysis reveals that local neighborhood specifications cover *zero* test images in the entire MNIST dataset with $\epsilon = 0.2$, which is the maximum L_∞ verifiable bound used in VNNCOMP [Brix et al. 2023], the annual neural network verification competition. This further validates our motivation for using NAPs as specifications.

For instance, for label 0, OPTADVPRUNE detects 618 essential neurons and correctly identify 445 and 160 of the 480 neurons in the minimal NAP founded by COARSEN. When interacting with

Table 2. Overview of learned minimal NAP specifications on the MNIST benchmark.

	0					1					4				
	$ P $	$\#\mathcal{V}$	<i>train%</i>	<i>test%</i>	<i>vol.</i>	$ P $	$\#\mathcal{V}$	<i>train%</i>	<i>test%</i>	<i>vol.</i>	$ P $	$\#\mathcal{V}$	<i>train%</i>	<i>test%</i>	<i>vol.</i>
$\bar{\mathcal{A}}$ function (<i>baseline.</i>)	751	1	79.50	71.51	1	745	1	75.01	70.11	1	712	1	77.54	75.24	1
COARSEN	480	751	98.68	98.78	10^8	491	745	98.90	98.59	10^6	506	712	98.51	97.45	10^9
STOCHCOARSEN	532	33	93.19	93.01	10^5	559	27	94.12	93.68	10^3	562	25	93.89	93.64	10^6
OPTADVPRUNE	618	15	83.13	81.32	10^2	630	18	86.02	85.51	10^2	699	21	82.66	84.12	10^2

\mathcal{V} , OPTADVPRUNE computes minimal NAPs with an average of fewer than 20 calls. However, it experiences a decline in data coverage, with an average drop of over 5% compared to the baseline.

In summary, there is no universal solution to a given minimal specification problem. Our experiment highlights the distinct strengths and trade-offs of the three algorithms. While the results from all have guarantee on correctness, COARSEN finds the minimal NAP among the three, making it the most reliable for applications where rigorous minimality is priority. STOCHCOARSEN offers a significant speed advantage on top of COARSEN while maintaining minimality: the learned minimal NAP specification uses approximately 1.1x more neurons but requires only 5% of the verification calls. This significant reduction in computational overhead makes STOCHCOARSEN particularly well-suited for scenarios where efficiency is a priority. Finally, OPTADVPRUNE, employing an optimistic approach, is the fastest. The initial set of neurons, when they can be successfully verified, provides a tight upper bound for the global minimum. When the initial set cannot be verified, it provides an effective starting point for STOCHCOARSEN and COARSEN. Moreover, OPTADVPRUNE can be utilized in a verification-dependent manner, they excel in scenarios that scale beyond our verification capabilities. In these situations, they provide accurate estimations of essential neurons, enabling us to examine potential causal links between neurons and the interpretability and robustness of deep neural networks, as we will illustrate in the next experiment. Together, these algorithms apply to diverse scenarios, allowing users to balance speed and minimality accuracy, and guarantee of validity based on their specific requirements.

6.3 ImageNet with Deep Convolutional Neural Network

In our third experiment, we present our finds on the fully connected layers¹ of VGG-19 network pretrained on the ImageNet dataset, consisting of 8192 neurons. Provided it is currently impossible to verify NAP specifications on models of this size, we focus on analyzing the effect of essential neurons estimated using OPTADVPRUNE. We also limit our analysis to the top five largest classes, each containing approximately 1000 training and 350 test images. Our findings indicate that these estimated NAPs cover a significant portion of unseen test data, highlighting their potential as robust certificates for the test set. More details can be found in Appendix B.

NAP Captures Visual Interpretability and Inherent Robustness. From the perspective of representation learning, neural networks acquire both low- and high-level feature extractors, which they use to make final classification decisions based on hidden features (neuron representations) [Bengio et al. 2013]. Therefore, the robustness and consistency of a model’s predictions are influenced by the quality of these learned features. In essence, achieving an accurate and robust model hinges on learning "good" hidden representations, which are characterized by better interpretability [Zhang et al. 2021]. Many studies suggest a close relationship between visual interpretability and robustness, often observed in the learned features and representations [Alvarez Melis and Jaakkola 2018; Boopathy et al. 2020; Dong et al. 2017]. Thus, although we cannot yet formally verify the correctness of these estimated NAP specifications, we demonstrate that these NAPs are indeed "meaningful" through visual interpretability—strong evidence that the estimated essential neurons (NAPs) contribute to the model’s robustness.

To this end, we make a simple modification to Grad-CAM [Selvaraju et al. 2017], which highlights key regions of an input image by using the gradients of the classification score with respect to the final convolutional feature map. Specifically, we mask out the neurons that do not appear in NAP in the fully connected layers. We then recalculate the backward gradient flow using this modified computation graph to generate the updated Grad-CAM map. Finally, we conduct the following experiments on image samples:

¹NAP computation for convolutional layers is left for future work.

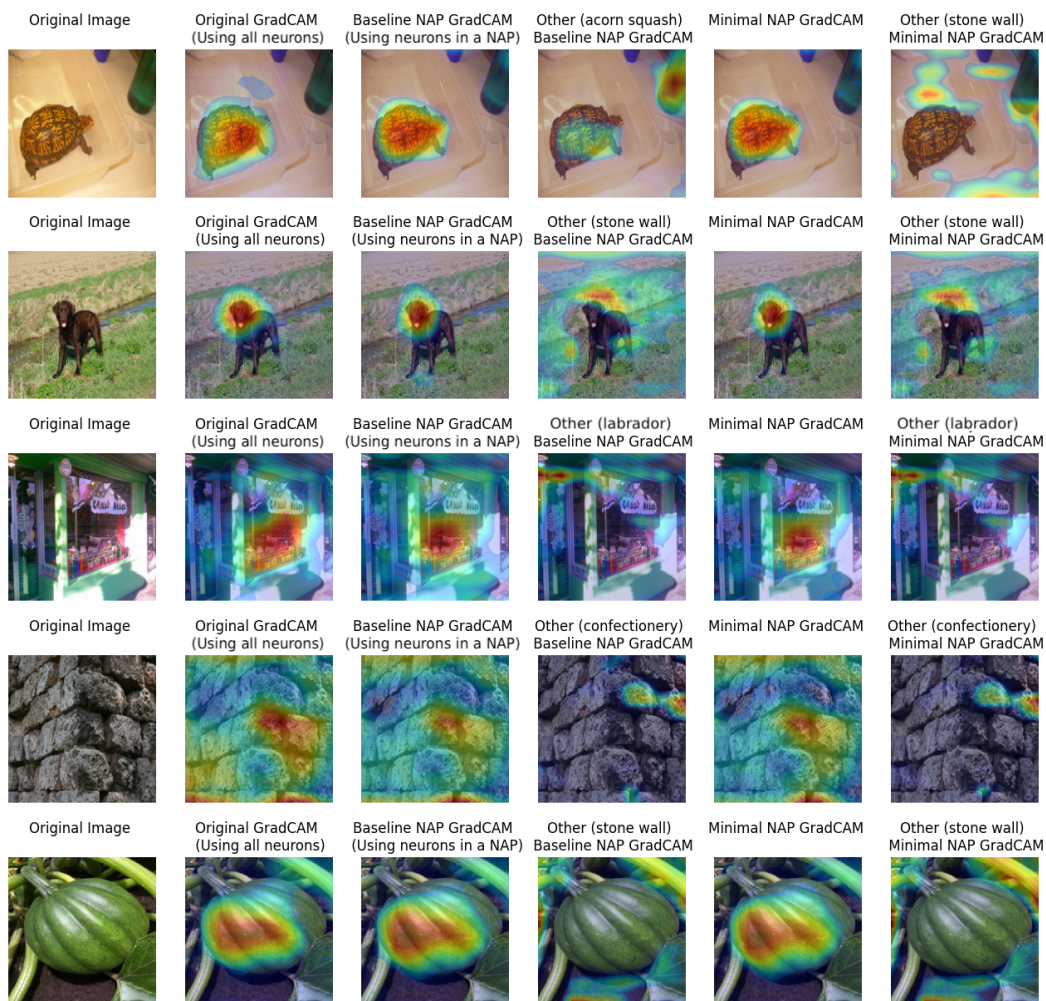


Fig. 6. Visual interpretability of learned hidden representations retained by estimated NAPs. The first two columns represent the original images and GradCams, respectively. The third and fourth columns represent modified GradCams using baseline NAPs of the same class and another class, respectively. The last two columns represent modified GradCams using minimal NAPs of the same class and another class, respectively.

- (1) Calculate the modified Grad-CAM map using the most refined (baseline) NAP and compare it with the original Grad-CAM map.
- (2) Calculate the modified Grad-CAM map using minimal NAPs estimated by OPTADVPRUNE, and compare it with the original map.
- (3) Calculate the modified Grad-CAM map using NAPs from different classes and compare it with the original map.

All GradCam maps are further validated with sanity checks [Adebayo et al. 2018]. Figure 6 presents the experimental results. The original GradCams highlight important regions of images corresponding to crucial justifications for classification. Notably, both the most refined and estimated minimal NAPs produce nearly identical highlights, despite representing only a small fraction of

neurons. This shows that the neuron abstractions from our minimal specification preserve the key visual features. Further, it suggests that the estimated minimal NAPs capture crucial aspects of VGG-19’s internal decision-making process, supporting the "NAP robustness property." Furthermore, Grad-CAMs generated from NAPs of different classes highlight distinct regions, strongly indicating that our estimated NAPs are clearly distinguishable, aligning with the "non-ambiguity property."

These results demonstrate that NAPs offer valuable insights into interpretability. A small subset of neurons from NAPs can categorize critical internal dynamics of neural networks, potentially helping us unveil the black-box nature of these systems. From a machine-checkable definition perspective, concise NAPs are easier to decode into human-understandable programs than more refined NAPs. This underscores the importance of learning minimal NAPs. Interpreting NAPs into human-readable formats remains a direction for future research.

NAP as a Defense Against Adversarial Attacks. From a practical point of view, we believe that even before 1) formal verification finally scales; and/or 2) NAPs are fully interpretable, NAPs, as they are now, can already serve as an empirical certificate of a prediction or some defense mechanism, as shown in recent work [Lukina et al. 2021]. In the same spirit, we demonstrate that our estimated essential neurons can serve as defense against adversarial attacks.

We first select images that meet two criteria: 1) correctly predicted by the model; and 2) covered by the respective NAP. On average, each NAP covers approximately 40% of the training data of the corresponding class. For each selected image, we generate 100 distinct adversarial examples that are misclassified by the model, using Projected Gradient Descent attack [Madry et al. 2018] and Carlini Wagner attack [Carlini and Wagner 2017] respectively. We then check whether each adversarial image’s activation pattern is rejected by the respective NAPs. If so, we conclude that NAPs can empirically serve as specifications; Otherwise, they are proven to be not robust. Notably, we find that both the baseline NAPs and the estimated minimal NAPs reject all adversarial examples, indicating their effectiveness in describing a safe region and their potential as certificates.

7 RELATED WORK

7.1 Neural Network Verification

Neural network verification has attracted much attention due to the increasingly widespread applications of neural networks in safety-critical systems. its NP-hard nature resulting from the non-convexity introduced by activation functions [Katz et al. 2017b] makes it a challenging task. Thus most of the existing work on neural network verification focuses on designing scalable verification algorithms. For instance, while initially proposed solver-based approaches [Cheng et al. 2017; Ehlers 2017; Huang et al. 2017b; Tjeng et al. 2019] were limited to verify small neural networks with fewer than 100 neurons, state-of-the-art methods [Lu and Kumar 2019; Wang et al. 2021c; Xu et al. 2021] can verify more complex neural networks. It is worth mentioning that most existing work adopts local neighborhood specifications to verify the robustness properties of neural networks [Shapira et al. 2023]. Despite being a reliable measure, using local neighborhood specifications around reference data points may not cover any test data, let alone generalizing to the verification of unseen test set data. Geng et al. [2023] propose the new paradigm of NAP specifications to address this challenge. Our work advances the understanding of NAP specifications.

7.2 Abstract Interpretation

Abstract interpretation [Cousot and Cousot 1977] is a fundamental concept in software analysis and verification, particularly for approximating the semantics of discrete program states. By sacrificing precision, abstract interpretation typically enables scalable and faster proof finding during verification [Cousot and Cousot 2014]. Although abstract interpretation for neural network

verification has been proposed and studied in previous literature [Gehr et al. 2018; Mirman et al. 2018], abstract interpretation of neural activation patterns for verification is a relatively new field. Perhaps the most related work from the perspective of abstract interpretation is learning minimal abstractions [Liang et al. 2011]. While our work shares similarities in problem formulation and statistical approaches, we address fundamentally different problems. One limitation in our work is that our abstraction states may be too coarse: value in range $(0, +\infty)$ is abstracted into one state. This approach could over-approximate neuron behavior and thus fail to prove certain properties. We observe that neuron values exhibit different patterns in range for different input classes, suggesting the potential existence of more abstraction states. We leave this as future work.

7.3 Neural Activation Patterns

Neural activation patterns have commonly been used to understand the internal decision-making process of neural networks. One popular line of research is feature visualization [Bauerle et al. 2022; Yosinski et al. 2015], which investigates which neurons are activated or deactivated given different inputs. This is also naturally related to the field of activation maximization [Simonyan et al. 2014], which studies what kind of inputs could mostly activate certain neurons in the neural network. In this way, certain prediction outcomes may be attributed to the behavior of specific neurons, thereby increasing the interpretability of the underlying models. Lukina et al. [2021] demonstrates that neural activation patterns can be used to monitor neural networks and detect novel or unknown input classes at runtime. They provide human-level interpretability of neural network decision-making. In summary, most of existing works focus on learning statistical correlations between NAPs and inputs [Bau et al. 2017; Erhan et al. 2009], or between NAPs and prediction outcomes [Lukina et al. 2021]. However, these correlations raises questions which we address in this paper: whether the correlation can be trusted or even verified. We propose the concept of essential neurons and highlight their importance in the robustness of model predictions. Such causal links between neurons and prediction outcomes are not only identified but also verified. We believe this "identify then verify" paradigm can be extended to existing research on NAPs to certify our understanding of neural networks. We leave the exploration of this direction for our future work.

8 CONCLUSION

We introduce a new challenge: learning the minimal NAP specification and highlighting its significance in neural network verification. Identifying minimal NAP specifications not only facilitates the verification of larger input regions compared to existing methods but also provides insights into when and how neural networks make reliable and robust predictions. To address this problem, we propose three approaches—conservative, statistical, and optimistic—each offering distinct trade-offs between efficiency and performance. The first two rely on the verification tool to find minimal NAP specifications. The optimistic method efficiently estimates minimal NAPs using adversarial examples, without making calls to the verification tool until the very end. Each of these methods offers distinct strengths and trade-offs in terms of minimality and computational speed, making each approach suitable for scenarios with different priorities. The learnt minimal NAP specification allows us to inspect potential causal links between neurons and the robustness of state-of-the-art neural networks, a task for which existing work fails to scale. Our experimental results suggest that minimal NAP specifications require much smaller fractions of neurons compared to the NAP specifications computed by previous work, yet they can significantly expand the verifiable boundaries to several orders of magnitude larger.

REFERENCES

- Julius Adebayo, Justin Gilmer, Michael Muelly, Ian Goodfellow, Moritz Hardt, and Been Kim. 2018. Sanity checks for saliency maps. *Advances in neural information processing systems* 31 (2018).
- David Alvarez Melis and Tommi Jaakkola. 2018. Towards robust interpretability with self-explaining neural networks. *Advances in neural information processing systems* 31 (2018).
- David Bau, Bolei Zhou, Aditya Khosla, Aude Oliva, and Antonio Torralba. 2017. Network Dissection: Quantifying Interpretability of Deep Visual Representations. In *2017 IEEE Conference on Computer Vision and Pattern Recognition, CVPR 2017, Honolulu, HI, USA, July 21-26, 2017*. IEEE Computer Society, 3319–3327. <https://doi.org/10.1109/CVPR.2017.354>
- Alex Bäuerle, Daniel Jönsson, and Timo Ropinski. 2022. Neural Activation Patterns (NAPs): Visual Explainability of Learned Concepts. *CoRR* abs/2206.10611 (2022). <https://doi.org/10.48550/arXiv.2206.10611> arXiv:2206.10611
- Yoshua Bengio, Aaron Courville, and Pascal Vincent. 2013. Representation Learning: A Review and New Perspectives. *IEEE Transactions on Pattern Analysis and Machine Intelligence* 35, 8 (2013), 1798–1828. <https://doi.org/10.1109/TPAMI.2013.50>
- Akhilan Boopathy, Sijia Liu, Gaoyuan Zhang, Cynthia Liu, Pin-Yu Chen, Shiyu Chang, and Luca Daniel. 2020. Proper network interpretability helps adversarial robustness in classification. In *International Conference on Machine Learning*. PMLR, 1014–1023.
- Christopher Brix, Stanley Bak, Changliu Liu, and Taylor T. Johnson. 2023. The Fourth International Verification of Neural Networks Competition (VNN-COMP 2023): Summary and Results. *CoRR* abs/2312.16760 (2023). <https://doi.org/10.48550/ARXIV.2312.16760> arXiv:2312.16760
- N. Carlini and D. Wagner. 2017. Towards Evaluating the Robustness of Neural Networks. In *2017 IEEE Symposium on Security and Privacy (SP)*. IEEE Computer Society, Los Alamitos, CA, USA, 39–57. <https://doi.org/10.1109/SP.2017.49>
- Chih-Hong Cheng, Georg Nührenberg, and Harald Ruess. 2017. Maximum Resilience of Artificial Neural Networks. In *Automated Technology for Verification and Analysis - 15th International Symposium, ATVA 2017, Pune, India, October 3-6, 2017, Proceedings (Lecture Notes in Computer Science, Vol. 10482)*, Deepak D’Souza and K. Narayan Kumar (Eds.). Springer, 251–268. https://doi.org/10.1007/978-3-319-68167-2_18
- Patrick Cousot and Radhia Cousot. 1977. Abstract Interpretation: A Unified Lattice Model for Static Analysis of Programs by Construction or Approximation of Fixpoints. In *Conference Record of the Fourth ACM Symposium on Principles of Programming Languages, Los Angeles, California, USA, January 1977*, Robert M. Graham, Michael A. Harrison, and Ravi Sethi (Eds.). ACM, 238–252. <https://doi.org/10.1145/512950.512973>
- Patrick Cousot and Radhia Cousot. 2014. Abstract interpretation: past, present and future. In *Joint Meeting of the Twenty-Third EACSL Annual Conference on Computer Science Logic (CSL) and the Twenty-Ninth Annual ACM/IEEE Symposium on Logic in Computer Science (LICS), CSL-LICS ’14, Vienna, Austria, July 14 - 18, 2014*, Thomas A. Henzinger and Dale Miller (Eds.). ACM, 2:1–2:10. <https://doi.org/10.1145/2603088.2603165>
- Thomas G. Dietterich and Eric Horvitz. 2015. Rise of concerns about AI: reflections and directions. *Commun. ACM* 58, 10 (2015), 38–40. <https://doi.org/10.1145/2770869>
- Yinpeng Dong, Hang Su, Jun Zhu, and Fan Bao. 2017. Towards interpretable deep neural networks by leveraging adversarial examples. *arXiv preprint arXiv:1708.05493* (2017).
- Martin E. Dyer and Alan M. Frieze. 1988. On the Complexity of Computing the Volume of a Polyhedron. *SIAM J. Comput.* 17, 5 (1988), 967–974. <https://doi.org/10.1137/0217060>
- Rüdiger Ehlers. 2017. Formal Verification of Piece-Wise Linear Feed-Forward Neural Networks. *CoRR* abs/1705.01320 (2017). arXiv:1705.01320 <http://arxiv.org/abs/1705.01320>
- D. Erhan, Yoshua Bengio, Aaron C. Courville, and Pascal Vincent. 2009. Visualizing Higher-Layer Features of a Deep Network.
- Jonathan Frankle and Michael Carbin. 2019. The Lottery Ticket Hypothesis: Finding Sparse, Trainable Neural Networks. In *7th International Conference on Learning Representations, ICLR 2019, New Orleans, LA, USA, May 6-9, 2019*. OpenReview.net. <https://openreview.net/forum?id=rjl-b3RcF7>
- Timon Gehr, Matthew Mirman, Dana Drachler-Cohen, Petar Tsankov, Swarat Chaudhuri, and Martin Vechev. 2018. AI2: Safety and Robustness Certification of Neural Networks with Abstract Interpretation. In *2018 IEEE Symposium on Security and Privacy (SP)*. 3–18. <https://doi.org/10.1109/SP.2018.00058>
- Chuqin Geng, Nham Le, Xiaojie Xu, Zhaoyue Wang, Arie Gurfinkel, and Xujie Si. 2023. Towards Reliable Neural Specifications. In *International Conference on Machine Learning, ICML 2023, 23-29 July 2023, Honolulu, Hawaii, USA (Proceedings of Machine Learning Research, Vol. 202)*, Andreas Krause, Emma Brunskill, Kyunghyun Cho, Barbara Engelhardt, Sivan Sabato, and Jonathan Scarlett (Eds.). PMLR, 11196–11212. <https://proceedings.mlr.press/v202/geng23a.html>
- Chuqin Geng, Xiaojie Xu, Haolin Ye, and Xujie Si. 2022. Scalar Invariant Networks with Zero Bias. *CoRR* abs/2211.08486 (2022). <https://doi.org/10.48550/ARXIV.2211.08486> arXiv:2211.08486
- Ian J. Goodfellow, Jonathon Shlens, and Christian Szegedy. 2015. Explaining and Harnessing Adversarial Examples. In *3rd International Conference on Learning Representations, ICLR 2015, San Diego, CA, USA, May 7-9, 2015, Conference Track Proceedings*, Yoshua Bengio and Yann LeCun (Eds.). <http://arxiv.org/abs/1412.6572>

- Divya Gopinath, Kaiyuan Wang, Mengshi Zhang, Corina S. Pasareanu, and Sarfraz Khurshid. 2018. Symbolic Execution for Deep Neural Networks. *CoRR* abs/1807.10439 (2018). arXiv:1807.10439 <http://arxiv.org/abs/1807.10439>
- Boris Hanin and David Rolnick. 2019a. Complexity of Linear Regions in Deep Networks. In *ICML (Proceedings of Machine Learning Research, Vol. 97)*. PMLR, 2596–2604.
- Boris Hanin and David Rolnick. 2019b. Deep ReLU Networks Have Surprisingly Few Activation Patterns. In *NeurIPS*. 359–368.
- Xiaowei Huang, Daniel Kroening, Wenjie Ruan, James Sharp, Youcheng Sun, Emese Thamo, Min Wu, and Xinpeng Yi. 2020. A survey of safety and trustworthiness of deep neural networks: Verification, testing, adversarial attack and defence, and interpretability. *Comput. Sci. Rev.* 37 (2020), 100270. <https://doi.org/10.1016/j.cosrev.2020.100270>
- Xiaowei Huang, Marta Kwiatkowska, Sen Wang, and Min Wu. 2017a. Safety Verification of Deep Neural Networks. In *Computer Aided Verification - 29th International Conference, CAV 2017, Heidelberg, Germany, July 24-28, 2017, Proceedings, Part I (Lecture Notes in Computer Science, Vol. 10426)*, Rupak Majumdar and Viktor Kuncak (Eds.). Springer, 3–29. https://doi.org/10.1007/978-3-319-63387-9_1
- Xiaowei Huang, Marta Kwiatkowska, Sen Wang, and Min Wu. 2017b. Safety Verification of Deep Neural Networks. In *Computer Aided Verification - 29th International Conference, CAV 2017, Heidelberg, Germany, July 24-28, 2017, Proceedings, Part I (Lecture Notes in Computer Science, Vol. 10426)*, Rupak Majumdar and Viktor Kuncak (Eds.). Springer, 3–29. https://doi.org/10.1007/978-3-319-63387-9_1
- Guy Katz, Clark Barrett, David Dill, Kyle Julian, and Mykel Kochenderfer. 2017a. Reluplex: An Efficient SMT Solver for Verifying Deep Neural Networks. arXiv:1702.01135 [cs.AI] <https://arxiv.org/abs/1702.01135>
- Guy Katz, Clark W. Barrett, David L. Dill, Kyle Julian, and Mykel J. Kochenderfer. 2017b. Reluplex: An Efficient SMT Solver for Verifying Deep Neural Networks. In *Computer Aided Verification - 29th International Conference, CAV 2017, Heidelberg, Germany, July 24-28, 2017, Proceedings, Part I (Lecture Notes in Computer Science, Vol. 10426)*, Rupak Majumdar and Viktor Kuncak (Eds.). Springer, 97–117. https://doi.org/10.1007/978-3-319-63387-9_5
- Guy Katz, Derek A. Huang, Duligur Ibeling, Kyle Julian, Christopher Lazarus, Rachel Lim, Parth Shah, Shantanu Thakoor, Haoze Wu, Aleksandar Zeljic, David L. Dill, Mykel J. Kochenderfer, and Clark W. Barrett. 2019. The Marabou Framework for Verification and Analysis of Deep Neural Networks. In *Computer Aided Verification - 31st International Conference, CAV 2019, New York City, NY, USA, July 15-18, 2019, Proceedings, Part I (Lecture Notes in Computer Science, Vol. 11561)*, Isil Dillig and Sedar Tasiran (Eds.). Springer, 443–452. https://doi.org/10.1007/978-3-030-25540-4_26
- Zhaoyu Li, Jinpei Guo, Yuhe Jiang, and Xujie Si. 2023. Learning Reliable Logical Rules with SATNet. In *Advances in Neural Information Processing Systems 36: Annual Conference on Neural Information Processing Systems 2023, NeurIPS 2023, New Orleans, LA, USA, December 10 - 16, 2023*, Alice Oh, Tristan Naumann, Amir Globerson, Kate Saenko, Moritz Hardt, and Sergey Levine (Eds.). http://papers.nips.cc/paper_files/paper/2023/hash/2ff46d83d1dcc063e075058b29d55efe-Abstract-Conference.html
- Percy Liang, Omer Tripp, and Mayur Naik. 2011. Learning minimal abstractions. In *Proceedings of the 38th ACM SIGPLAN-SIGACT Symposium on Principles of Programming Languages, POPL 2011, Austin, TX, USA, January 26-28, 2011*, Thomas Ball and Mooly Sagiv (Eds.). ACM, 31–42. <https://doi.org/10.1145/1926385.1926391>
- Tailin Liang, John Glossner, Lei Wang, Shaobo Shi, and Xiaotong Zhang. 2021. Pruning and quantization for deep neural network acceleration: A survey. *Neurocomputing* 461 (2021), 370–403. <https://doi.org/10.1016/j.NEUCOM.2021.07.045>
- Jingyue Lu and M. Pawan Kumar. 2019. Neural Network Branching for Neural Network Verification. *CoRR* abs/1912.01329 (2019). arXiv:1912.01329 <http://arxiv.org/abs/1912.01329>
- Lu Lu, Yeonjong Shin, Yanhui Su, and George E. Karniadakis. 2019. Dying ReLU and Initialization: Theory and Numerical Examples. *CoRR* abs/1903.06733 (2019). arXiv:1903.06733 <http://arxiv.org/abs/1903.06733>
- Anna Lukina, Christian Schilling, and Thomas A. Henzinger. 2021. Into the Unknown: Active Monitoring of Neural Networks. In *Runtime Verification - 21st International Conference, RV 2021, Virtual Event, October 11-14, 2021, Proceedings (Lecture Notes in Computer Science, Vol. 12974)*, Lu Feng and Dana Fisman (Eds.). Springer, 42–61. https://doi.org/10.1007/978-3-030-88494-9_3
- Aleksander Madry, Aleksandar Makelov, Ludwig Schmidt, Dimitris Tsipras, and Adrian Vladu. 2018. Towards Deep Learning Models Resistant to Adversarial Attacks. In *6th International Conference on Learning Representations, ICLR 2018, Vancouver, BC, Canada, April 30 - May 3, 2018, Conference Track Proceedings*. OpenReview.net. <https://openreview.net/forum?id=rjzIBfZAb>
- Matthew Mirman, Timon Gehr, and Martin T. Vechev. 2018. Differentiable Abstract Interpretation for Provably Robust Neural Networks. In *International Conference on Machine Learning*. <https://api.semanticscholar.org/CorpusID:51872670>
- Ramprasaath R. Selvaraju, Abhishek Das, Ramakrishna Vedantam, Michael Cogswell, Devi Parikh, and Dhruv Batra. 2017. Grad-CAM: Visual Explanations from Deep Networks via Gradient-Based Localization. In *2017 IEEE International Conference on Computer Vision (ICCV)*. 618–626. <https://doi.org/10.1109/ICCV.2017.74>
- Yuval Shapira, Eran Avneri, and Dana Drachler-Cohen. 2023. Deep Learning Robustness Verification for Few-Pixel Attacks. *Proc. ACM Program. Lang.* 7, OOPSLA1, Article 90 (apr 2023), 28 pages. <https://doi.org/10.1145/3586042>

- Karen Simonyan, Andrea Vedaldi, and Andrew Zisserman. 2014. Deep Inside Convolutional Networks: Visualising Image Classification Models and Saliency Maps. In *2nd International Conference on Learning Representations, ICLR 2014, Banff, AB, Canada, April 14-16, 2014, Workshop Track Proceedings*, Yoshua Bengio and Yann LeCun (Eds.). <http://arxiv.org/abs/1312.6034>
- Karen Simonyan and Andrew Zisserman. 2014. Very Deep Convolutional Networks for Large-Scale Image Recognition. *CoRR* abs/1409.1556 (2014). <https://api.semanticscholar.org/CorpusID:14124313>
- Naftali Tishby and Noga Zaslavsky. 2015. Deep learning and the information bottleneck principle. In *2015 IEEE Information Theory Workshop (ITW)*. IEEE, 1–5.
- Vincent Tjeng, Kai Yuanqing Xiao, and Russ Tedrake. 2019. Evaluating Robustness of Neural Networks with Mixed Integer Programming. In *7th International Conference on Learning Representations, ICLR 2019, New Orleans, LA, USA, May 6-9, 2019*. OpenReview.net. <https://openreview.net/forum?id=HyGIdiRqtm>
- VNNCOMP. 2021. VNNCOMP. <https://sites.google.com/view/vnn2021>
- Shiqi Wang, Huan Zhang, Kaidi Xu, Xue Lin, Suman Jana, Cho-Jui Hsieh, and J. Zico Kolter. 2021b. Beta-CROWN: Efficient Bound Propagation with Per-neuron Split Constraints for Neural Network Robustness Verification. In *Advances in Neural Information Processing Systems 34: Annual Conference on Neural Information Processing Systems 2021, NeurIPS 2021, December 6-14, 2021, virtual*, Marc’Aurelio Ranzato, Alina Beygelzimer, Yann N. Dauphin, Percy Liang, and Jennifer Wortman Vaughan (Eds.). 29909–29921. <https://proceedings.neurips.cc/paper/2021/hash/fac7fead96dafceaf80c1daffae82a4-Abstract.html>
- Shiqi Wang, Huan Zhang, Kaidi Xu, Xue Lin, Suman Jana, Cho-Jui Hsieh, and J. Zico Kolter. 2021c. Beta-CROWN: Efficient Bound Propagation with Per-neuron Split Constraints for Neural Network Robustness Verification. In *Advances in Neural Information Processing Systems 34: Annual Conference on Neural Information Processing Systems 2021, NeurIPS 2021, December 6-14, 2021, virtual*, Marc’Aurelio Ranzato, Alina Beygelzimer, Yann N. Dauphin, Percy Liang, and Jennifer Wortman Vaughan (Eds.). 29909–29921. <https://proceedings.neurips.cc/paper/2021/hash/fac7fead96dafceaf80c1daffae82a4-Abstract.html>
- Zi Wang, Chengcheng Li, and Xiangyang Wang. 2021a. Convolutional Neural Network Pruning With Structural Redundancy Reduction. In *IEEE Conference on Computer Vision and Pattern Recognition, CVPR 2021, virtual, June 19-25, 2021*. Computer Vision Foundation / IEEE, 14913–14922. <https://doi.org/10.1109/CVPR46437.2021.01467>
- Jeanette M. Wing. 1990. A Specifier’s Introduction to Formal Methods. *Computer* 23, 9 (1990), 8–24. <https://doi.org/10.1109/2.58215>
- William Wolberg, Olvi Mangasarian, Nick Street, and W. Street. 1995. Breast Cancer Wisconsin (Diagnostic). UCI Machine Learning Repository. DOI: <https://doi.org/10.24432/C5DW2B>.
- Han Xu, Yao Ma, Haochen Liu, Debayan Deb, Hui Liu, Jiliang Tang, and Anil K. Jain. 2020. Adversarial Attacks and Defenses in Images, Graphs and Text: A Review. *Int. J. Autom. Comput.* 17, 2 (2020), 151–178. <https://doi.org/10.1007/s11633-019-1211-x>
- Kaidi Xu, Huan Zhang, Shiqi Wang, Yihan Wang, Suman Jana, Xue Lin, and Cho-Jui Hsieh. 2021. Fast and Complete: Enabling Complete Neural Network Verification with Rapid and Massively Parallel Incomplete Verifiers. In *9th International Conference on Learning Representations, ICLR 2021, Virtual Event, Austria, May 3-7, 2021*. OpenReview.net. <https://openreview.net/forum?id=nVZtXBI6LNn>
- Jason Yosinski, Jeff Clune, Anh Mai Nguyen, Thomas J. Fuchs, and Hod Lipson. 2015. Understanding Neural Networks Through Deep Visualization. *CoRR* abs/1506.06579 (2015). arXiv:1506.06579 <http://arxiv.org/abs/1506.06579>
- Yu Zhang, Peter Tiño, Ales Leonardis, and Ke Tang. 2021. A Survey on Neural Network Interpretability. *IEEE Trans. Emerg. Top. Comput. Intell.* 5, 5 (2021), 726–742. <https://doi.org/10.1109/TETCI.2021.3100641>

A LEARNED MINIMAL NAP SPECIFICATIONS ON THE MNIST BENCHMARK (COMPLEMENT)

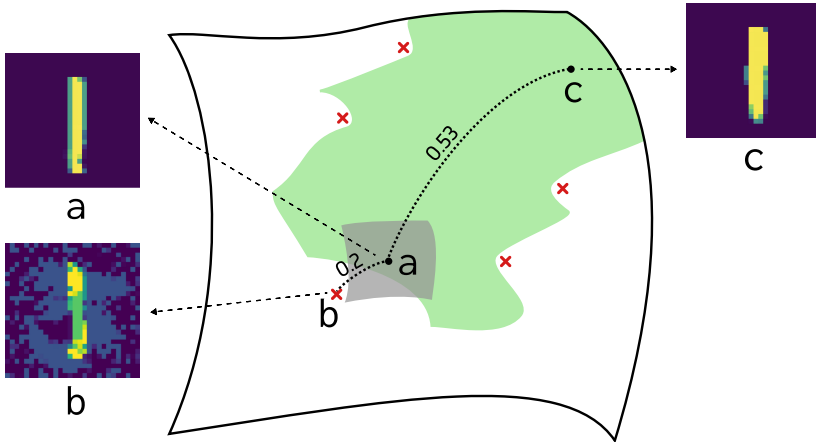


Fig. 7. The comparison between NAP specifications (green region) and L_∞ ball specifications (gray region) on the MNIST dataset. Image a is the reference image, and image c is the closest among all 6000 training images of digit 1, with an L_∞ distance of 0.5294. However, c cannot be verified using the L_∞ ball specification, as an adversarial example b exists at an L_∞ distance of 0.2. Note that this is not a limitation of the underlying verification engines but rather an intrinsic limitation of the specifications. In contrast, NAP specifications allow verification of unseen test set data like c .

Table 3. Overview of the size of learned minimal NAP specifications on the MNIST benchmark.

	2				3				5				6			
	$ P $	$\#\mathcal{V}$	train	test	$ P $	$\#\mathcal{V}$	train	test	$ P $	$\#\mathcal{V}$	train	test	$ P $	$\#\mathcal{V}$	train	test
Baseline [Geng et al. 2023]	751	1	79.50	80.51	745	1	86.01	85.11	712	1	77.54	80.24	712	1	77.54	80.24
COARSEN	480	751	98.68	98.78	491	745	98.90	98.59	506	712	98.51	97.45	503	708	98.81	98.39
STOCHCOARSEN	532	33	93.19	93.01	559	27	94.12	93.68	562	25	93.89	93.64	542	29	98.81	98.39
OPTADVPRUNE	618	15	83.13	71.32	630	18	79.02	76.51	699	21	82.66	84.12	681	20	85.98	87.63

B LEARNED MINIMAL NAP SPECIFICATIONS ON IMAGENET WITH DEEP CONVOLUTIONAL NEURAL NETWORK (COMPLEMENT)

C THE REFINE APPROACHES

C.1 The Refine Approach

Conceptually, the REFINE approach iteratively increases the number of refined neurons in NAP P until $\mathcal{V}(P) = 1$, i.e., P is able to prove the underlying robustness query. In other words, we gradually increase the size parameter k and iterate over each NAP P of size k to check if $\mathcal{V}(P) = 1$, as illustrated in Algorithm 4. To determine if a solution to the problem exists, we first check if the most refined NAP can succeed in verification. We proceed to iterative refinement only if $\mathcal{V}(\bar{P}) = 1$. However, the algorithm is not efficient and requires $2^{|N|} - 1$ calls to \mathcal{V} in the worst case, as proven in Theorem C.1. Please refer to the proof in Appendix D. Therefore REFINE is only practical when the search space of the NAP family \mathcal{P} is small.

Theorem C.1. *The algorithm REFINE returns a minimal NAP specification with $O(2^{|N|})$ calls to \mathcal{V} .*

Table 4. Overview of the size of learned minimal NAP specifications on the MNIST benchmark.

	7				8				9			
	$ P $	$\#\mathcal{V}$	train	test	$ P $	$\#\mathcal{V}$	train	test	$ P $	$\#\mathcal{V}$	train	test
The $\tilde{\mathcal{A}}$ function	751	1	79.50	80.51	745	1	86.01	85.11	712	1	77.54	80.24
COARSEN	480	751	98.68	98.78	491	745	98.90	98.59	506	712	98.51	97.45
ADVERSARIAL_PRUNE	618	15	83.13	71.32	630	18	79.02	76.51	699	21	82.66	84.12
SAMPLE_COARSEN	532	33	93.19	93.01	559	27	94.12	93.68	562	25	93.89	93.64

Table 5. Overview of the size of learned minimal NAP specifications on the ImageNet benchmark.

	box_turtle		labrador_retriever		acorn_squash		confectionery		stone_wall	
	$ P $	test	$ P $	test	$ P $	test	$ P $	test	$ P $	test
The $\tilde{\mathcal{A}}$ function	1978	39.42	691	39.61	1003	29.23	878	33.84	971	31.54
ADVERSARIAL_PRUNE	1863	39.42	661	41.28	823	25.68	845	23.07	865	39.61
GRADIENT_SEARCH	611	53.30	572	87.01	301	52.40	256	44.23	260	54.90

Algorithm 4: REFINE

Input: The neural network N
Output: A minimal NAP specification P

```

1 Function Refine( $N$ )
2    $P \leftarrow \tilde{\mathcal{A}}(N)$ 
3   if  $\mathcal{V}(P) == 0$  then
4     return None; /* Return None if even the most refined NAP fails verification */
5   else
6     for  $k$  from 1 to  $|N|$  do
7        $P \leftarrow \tilde{\mathcal{A}}(N)$  /* Refinement starts from the coarsest NAP  $\hat{P}$  */
8        $K\_comb \leftarrow \text{Pick\_}K\_Neurons(k, N)$  /* Returns all combinations of size  $k$  */
9       for  $comb$  in  $K\_comb$  do
10        for  $N_{i,l}$  in  $comb$  do
11           $P \leftarrow \tilde{\Delta}(N_{i,l})$  /* Refine neurons in the chosen combination */
12          if  $|\mathcal{V}(P)| == 1$  then
13            return  $P$  /* Found the minimal NAP */

```

C.2 The Statistical Refine Approach

essential neurons are crucial for forming NAP specifications, as their binary states play a critical role in determining the neural network’s robustness performance. We leverage this property to find essential neurons statistically. To be more specific, suppose we sample some NAPs P_1, P_2, \dots, P_n from the NAP family \mathcal{P} . For those NAPs that qualify as specifications (i.e., $\mathcal{V}(P) = 1$), essential neurons should appear more frequently in them than in those NAPs that fail the verification tool (i.e., $\mathcal{V}(P) = 0$).

Based on this insight, we propose an approach called SAMPLE_REFINE that relies on non-repetitive sampling to identify essential neurons for solving the minimal NAP problem. We start with the coarsest NAP and iteratively collect the most probable essential neurons. In every iteration, we sample k NAPs by refining unvisited neurons with some probability θ . The sampled NAPs are

then fed to the verification tool, and the neuron that appears most frequently in verifiable NAPs is the most probable essential neuron in this iteration. The neuron is marked as visited, and the process stops when either we collect s neurons (assuming that s is known), or the current essential neurons form a NAP specification P , i.e., $\mathcal{V}(P) = 1$. Finally, we return the learned NAP, obtained by applying $\tilde{\mathcal{A}}$ to the collected neurons. The algorithm 5 provides an overview of the above procedure.

It is worth noting that SAMPLE_REFINE doesn't guarantee correctness, as we may end up collecting only the s most probable essential neurons, which may not be sufficient to form a specification. Another concern regarding this algorithm is sampling efficiency, specifically the potential for the number of samples required to grow exponentially with the size of the minimal NAP specification s . To understand why this is problematic, consider a scenario where the only minimal NAP specification P consists of all essential neurons; in this case, all $|M|$ neurons must be selected for P to be learned. If θ is set to a constant value, then the expected number of samples needed to obtain the NAP specification is $(\frac{1}{\theta})^{|M|}$. To address this, we set $\theta = \left(\frac{|M|}{|M|+1}\right)^{|M|}$. This choice ensures that the sampling efficiency is polynomial in both $|M|$ and s , as proven in Theorem C.2. Please refer to the proof in the Appendix E. In addition, Theorem C.2 also shows that with high probability, a essential neuron will be found with $O(\log|N|)$ calls to \mathcal{V} .

Algorithm 5: SAMPLE_REFINE**Input:** The neural network N , the probability θ , sample size k , and the size s **Output:** A minimal NAP specification P

```

1 Function Sample_NAPs(unvisited,  $\theta$ )
2    $P \leftarrow \tilde{\mathcal{A}}(N)$  /* Use the coarsest NAP as a blank template */
3   for  $N_{i,l}$  in unvisited do
4      $rand \leftarrow \text{random}(0, 1)$ 
5     if  $rand \leq \theta$  then
6        $P \leftarrow \tilde{\Delta}(N_{i,l})$  /* Refine unvisited neurons using  $\tilde{\Delta}$  with probability  $\theta$  */
7   return  $P$ 

8 Function Sample_Refine(visited,  $\theta$ ,  $k$ ,  $s$ )
9   while  $|visited| < s$  and  $\mathcal{V}(P) == 0$  do
10     $unvisited \leftarrow N \setminus visited$ 
11     $ctr = \text{dict}()$  /* Create a counter for each neuron in unvisited */
12    for  $\_in$  range( $k$ ) do
13       $P \leftarrow \text{Sample\_NAPs}(unvisited, \theta)$  /* Sample  $k$  NAPs */
14      for  $N_{i,l}$  in unvisited do
15        if  $P_{i,l} == \tilde{\mathcal{A}}(N_{i,l})$  and  $\mathcal{V}(P) == 1$  then
16           $ctr[N_{i,l}] += 1$  /* Count successful NAPs for each neuron */
17       $N_{mad} \leftarrow \text{argmax}_{N_{i,l} \in unvisited} \{ctr[N_{i,l}]\}$  /* Pick potential essential neuron */
18       $visited \leftarrow visited \cup \{N_{mad}\}$ 
19   return  $\tilde{\mathcal{A}}(visited)$ 

20  $P \leftarrow \tilde{\mathcal{A}}(N)$ 
21 if  $\mathcal{V}(P) == 0$  then
22   return None /* Return None if the most refined NAP fails verification */
23 else
24   if heuristics then
25      $visited \leftarrow \text{Gradient\_Search}(N) \cap \text{Adversarial\_Prune}(N)$ 
26   else
27      $visited \leftarrow \emptyset$  /* Start from the coarsest NAP */
28    $\text{Sample\_Refine}(visited, \theta, k, s)$ 

```

Theorem C.2. With probability $\theta = |\binom{|M|}{|M|+1}|^{|M|}$, SAMPLE_REFINE has $1 - \delta$ probability of outputting a minimal NAP specification with $\Theta(|M|^2(\log |N| + \log(s/\delta)))$ examples each iteration and $O(s|M|^2(\log |N| + \log(s/\delta)))$ total calls to \mathcal{V} .

D PROOFS OF SIMPLE APPROACHES

Theorem D.1 (Property of REFINE). *The algorithm REFINE returns a minimal NAP specification with $O(2^{|N|})$ calls to \mathcal{V} .*

PROOF. Let P be the returned NAP. We prove this by contradiction. Suppose we can further refine P , meaning there exists a NAP P' such that $|P'| \leq |P|$ and $\mathcal{V}(P') = 1$. However, the algorithm states that any P' smaller than $|P|$ fails verification, which contradicts $\mathcal{V}(P') = 1$.

In the worst case, the NAP size k runs up to $|N|$. For each k , we need to check $\binom{|N|}{k}$ number of NAPs. In total, this number of NAPs we need to check is $\binom{|N|}{1} + \binom{|N|}{2} + \dots + \binom{|N|}{|N|} = 2^{|N|} - 1$ according to the binomial theorem, resulting in a runtime complexity of $O(2^{|N|})$.

□

Theorem D.2 (Property of COARSEN). *The algorithm COARSEN returns a minimal NAP specification with $O(|N|)$ calls to \mathcal{V} .*

PROOF. Let P be the NAP returned by COARSEN. Our goal is to show that any P' smaller than P results in $\mathcal{V}(P') = 0$. To construct such a smaller P' , we need to apply the refine action $\tilde{\Delta}$ on P through some neuron $N_{i,l}$, i.e., $P' := \tilde{\Delta}(N_{i,l}) = \tilde{\mathcal{A}}(N_{i,l}) \cup P \setminus P_{i,l}$. According to the algorithm, $\mathcal{V}(P') = 0$. In the worst case, the algorithm needs to iterate through each neuron in N , resulting in a runtime complexity of $O(|N|)$. □

E PROOFS OF STATISTICAL APPROACHES

Our proofs of properties of SAMPLE_REFINE and SAMPLE_COARSEN mainly follow those in [Liang et al. 2011]. Interested readers may refer to it for detailed proofs.

Theorem E.1 (Property of SAMPLE_REFINE). *With probability $\theta = |(\frac{|M|}{|M|+1})|^{|M|}$, SAMPLE_REFINE has $1 - \delta$ probability of outputting a minimal NAP specification with $\Theta(|M|^2(\log |N| + \log(s/\delta)))$ examples each iteration and $O(s|M|^2(\log |N| + \log(s/\delta)))$ total calls to \mathcal{V} .*

PROOF. Considering the size of the minimal specification s , SAMPLE_REFINE will execute s iterations. If we sample k times in each iteration, then the probability of selecting a essential neuron is at least $1 - \frac{\delta}{s}$. Consequently, by applying a union bound, the algorithm will identify a NAP specification with a probability of at least $1 - \delta$.

Now, let's delve deeper into one iteration of the process. The fundamental concept is that a essential neuron m demonstrates a stronger correlation with proving the robustness query ($\mathcal{V}(P) = 1$) compared to a non-essential one. This enhanced correlation increases the probability of its selection significantly when k is sufficiently large.

Let's revisit the notion of M , representing the set of essential neurons with a size of $|M|$. Now, let's focus on a specific essential neuron $n^+ \in M$. We define B_{j-} as the event indicating $k_{n^-} > k_{n^+}$, and B as the event where B_{j-} holds for any non-essential neuron $n^- \in N \setminus M$. Importantly, if B fails to occur, then the algorithm will correctly identify a essential neuron. Hence, our primary objective is to establish that $Pr(B) \leq \frac{\delta}{s}$. Initially, employing a union bound provides:

$$Pr(B) \leq \sum_{n^-} Pr(B_{n^-}) \leq |N| \max_{n^-} Pr(B_{n^-}) \quad (15)$$

Let's delve into each training example $P^{(i)}$ and introduce the notation $X_i = (1 - \mathcal{V}(P^{(i)}))(P_{n^-}^{(i)} - P_{n^+}^{(i)})$. It's worth emphasizing that B_{n^-} manifests precisely when $\frac{1}{n}(k_{n^-} - k_{n^+}) = \frac{1}{n} \sum_{i=1}^n X_i > 0$. Our objective now is to bound this quantity utilizing Hoeffding's inequality, considering the mean as:

$$\mathbb{E}[X_i] = Pr(\mathcal{V}(P) = 1, P_{n^-} \in \{1, 0\}) - Pr(\mathcal{V}(P) = 1, P_{n^+} \in \{1, 0\}) \quad (16)$$

and the bounds are $-1 \leq \mathbb{E}[X_i] \leq 1$. Setting $\epsilon = -\mathbb{E}[X_i]$, we get:

$$Pr(B_{n^-}) \leq e^{-\frac{k\epsilon^2}{2}}, n^+ \in M, n^- \notin M. \quad (17)$$

Substituting (16) into (15) and rearranging terms, we can solve for k :

$$\frac{\delta}{s} \leq |N| e^{-\frac{k\epsilon^2}{2}} \text{ implies } k \geq \frac{2(\log |N| + \log(\frac{\delta}{s}))}{\epsilon^2} \quad (18)$$

Our attention now shifts towards deriving a lower bound for ϵ , which intuitively reflects the discrepancy (in terms of correlation with proving the robustness query) between a essential neuron and a non-essential one. It's noteworthy that $Pr(P_n \in \{1, 0\}) = \theta$ for any $n \in N$. Furthermore, since

n^- is non-essential, we can assert that $Pr(\mathcal{V}(P) = 1 | P_{n^-} \in \{1, 0\}) = Pr(\mathcal{V}(P) = 1)$. By leveraging these observations, we can express:

$$\epsilon = \theta(Pr(\mathcal{V}(P) = 1 | P_{n^+} \in \{1, 0\}) - Pr(\mathcal{V}(P) = 1)) \quad (19)$$

Let's view C as the collection of minimal NAP specifications. We can treat C as a set of clauses in a Disjunctive Normal Form (DNF) formula: $\mathcal{V}(P; C) = \neg \bigvee_{c \in C} \bigwedge_{n \in c} P_n$, where we explicitly specify the dependence of \mathcal{V} on the clauses C . For example, if $C = 1, 2, 3$, it corresponds to $\mathcal{V}(P) = \neg[(P_1 \wedge P_2) \vee P_3]$. Now, let $C_j = c \in C : n \in c$ denote the clauses containing n . We reformulate $Pr(\mathcal{V}(P) = 1)$ as the sum of two components: one originating from the essential neuron n^+ and the other from the non-essential neuron:

$$Pr(\mathcal{V}(P) = 1) = Pr(\mathcal{V}(P; C_{n^+}) = 1, \mathcal{V}(P; C \setminus C_{n^+}) = 0) \quad (20)$$

$$+ Pr(\mathcal{V}(P; C \setminus C_{n^+}) = 1) \quad (21)$$

Calculating $Pr(\mathcal{V}(P) = 1 | P_{n^+} \in \{1, 0\})$ follows a similar process. The only distinction arises from conditioning on $P_{n^+} \in \{1, 0\}$, which introduces an extra factor of $\frac{1}{\theta}$ in the first term because conditioning divides by $Pr(P_{n^+}) = \theta$. The second term remains unchanged since no $c \notin C_{n^+}$ is essential in P_{n^+} . Substituting these two outcomes back into the equation yields:

$$\epsilon = (1 - \theta)Pr(\mathcal{V}(P; C_{n^+}) = 1, \mathcal{V}(P; C \setminus C_{n^+}) = 0) \quad (22)$$

Now, our objective is to establish a lower bound for (22) across all possible \mathcal{V} (equivalently, C), where n^+ is permitted to be essential in C . Interestingly, the worst possible C can be obtained by either having $|M|$ disjoint clauses ($C = n : n \in M$) or a single clause ($C = M$ if $s = |M|$). The intuition behind this is that when C consists of $|M|$ clauses, there are numerous possibilities ($|M| - 1$ of them) for some $c \notin C_{n^+}$ to be true, making it challenging to determine that n^+ is an essential neuron; in such cases, $\epsilon = (1 - \theta)\theta(1 - \theta)^{|M|-1}$. Conversely, if C comprises a single clause, then letting this clause be true becomes exceedingly challenging; in this scenario, $\epsilon = (1 - \theta)\theta^{|M|}$.

Let's consider the scenario where C comprises $|M|$ clauses. We aim to maximize ϵ concerning θ by setting the derivative $\frac{d\epsilon}{d\theta} = 0$ and solving for θ . This optimization yields $\theta = \frac{1}{|M|+1}$ as the optimal value. Substituting this value into the formula of ϵ , we obtain $\epsilon = \frac{1}{|M|+1} \left(\frac{|M|}{|M|+1}\right)^{|M|}$. Note that $\left(\frac{|M|}{|M|+1}\right)^{|M|}$ can be lower bounded by e^{-1} , implying that $\epsilon^{-2} = \mathcal{O}(|M|^2)$. Substituting this result to equation (18) will conclude the proof. \square

Theorem E.2 (Property of STOCHASTIC_COARSEN). *With probability $\theta = e^{-\frac{1}{s}}$, SAMPLE_COARSEN learns a minimal NAP specification with $\mathcal{O}(s \log |N|)$ calls to \mathcal{V} .*

PROOF. Let's first estimate the number of calls that SAMPLE_COARSEN makes to \mathcal{V} . We denote the number of calls as $C(P^L)$, where P^L is the most refined NAP. Then $C(P^L)$ can be computed recursively using the following rule:

$$C(P^L) = \begin{cases} |P| & \text{if } |P^L| \leq s + 1 \\ 1 + \mathbb{E}[(1 - \mathcal{V}(P))C(P) + \mathcal{V}(P)C(P^L)] & \text{otherwise} \end{cases} \quad (23)$$

where P is the sampled NAP. By assumption, there exists a NAP $P^S \preceq P$ of size s that passes the verification. Define $G(P) = \neg(P^S \preceq P)$, which is 0 when P^S subsumes P , i.e., all essential neurons in P^S shows up in the sampled P . This follows that $Pr(G(P) = 0) = Pr(P^S \preceq P) = \theta^s$. Note that $G(P) \geq \mathcal{V}(P)$, as the NAP P^S suffices to prove the robustness query. We can estimate the upper

bound of $C(P^L)$ by replacing \mathcal{V} with G :

$$C(P^L) \leq 1 + \mathbb{E}[(1 - G(P))C(P) + G(P)C(P^L)] \quad (24)$$

$$\leq 1 + \theta^s \mathbb{E}[C(P)|P^S \leq P] + (1 - \theta^s)C(P^L) \quad (25)$$

$$\leq \mathbb{E}[C(P)|P^S \leq P] + \theta^{-s} \quad (26)$$

We now denote $C(n) = \max_{|P|=n} C(P)$ as the maximum over NAP of size n . Note that given $P^S \leq P$, $|P| = s + N$ where N is a binomial random variable with $\mathbb{E}(N) = \theta(n - s)$.

Using the bound $C(n) \leq (1 - \theta^n)C(n - 1) + \theta^n C(n)\theta^{-s}$, we can observe that $C(n) \leq \frac{\theta^{-s}}{1 - \theta^n} \cdot n$. In addition, when n is large enough, $C(n)$ is concave, then by use Jensen's inequality:

$$C(n) \leq C(\mathbb{E}[s + N]) + \theta^{-s} = C(s + \theta(n - s)) + \theta^{-s} \quad (27)$$

To solve the recurrence, this gives us:

$$C(n) \leq \frac{\theta^{-s} \log n}{\log \theta^{-1}} + s + 1 \quad (28)$$

The equation above illustrates a tradeoff between reducing the number of iterations (by increasing $\log \theta^{-1}$) and reducing the number of samples (by decreasing θ^{-s}). To minimize $C(n)$, we need to set θ so that the gradient of $C(n)$ w.r.t θ^{-1} is 0. This gives us: $\frac{sx^{s-1}}{\log x} - \frac{x^{s-1}}{\log^2 x} = 0$, solving this gives us $\theta = e^{-\frac{1}{s}}$. Consequently, the upper bound becomes $C(n) = es \log n + s + 1 = O(s \log n)$. \square

Received 20 February 2007; revised 12 March 2009; accepted 5 June 2009